

# Accepted Manuscript

Synthesis, Characterization, and Fiber-optic Infrared Reflectance Spectroelectrochemical Studies of Some Dinitrosyl Iron Diphosphine Complexes  $\text{Fe}(\text{NO})_2\text{L}_2$  ( $\text{L} = \text{P}(\text{C}_6\text{H}_4\text{X})_3$ )

Myron W. Jones, Douglas R. Powell, George B. Richter-Addo

PII: S0022-328X(13)00921-2

DOI: [10.1016/j.jorganchem.2013.12.040](https://doi.org/10.1016/j.jorganchem.2013.12.040)

Reference: JOM 18426

To appear in: *Journal of Organometallic Chemistry*

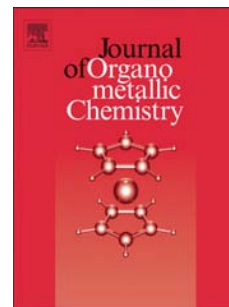
Received Date: 17 September 2013

Revised Date: 12 December 2013

Accepted Date: 20 December 2013

Please cite this article as: M.W. Jones, D.R. Powell, G.B. Richter-Addo, Synthesis, Characterization, and Fiber-optic Infrared Reflectance Spectroelectrochemical Studies of Some Dinitrosyl Iron Diphosphine Complexes  $\text{Fe}(\text{NO})_2\text{L}_2$  ( $\text{L} = \text{P}(\text{C}_6\text{H}_4\text{X})_3$ ), *Journal of Organometallic Chemistry* (2014), doi: 10.1016/j.jorganchem.2013.12.040.

This is a PDF file of an unedited manuscript that has been accepted for publication. As a service to our customers we are providing this early version of the manuscript. The manuscript will undergo copyediting, typesetting, and review of the resulting proof before it is published in its final form. Please note that during the production process errors may be discovered which could affect the content, and all legal disclaimers that apply to the journal pertain.



Graphical Abstract Synopsis:

Dinitrosyl iron complexes (DNICs) are important in biology and have utility in chemical catalysis. Several new DNICs of the form  $\text{Fe}(\text{NO})_2(\text{PAr}_3)_2$  ( $\text{PAr}_3$  = triarylphosphine) have been prepared and characterized by spectroscopy and X-ray crystallography. The results of the spectroscopy and electrochemistry reveal subtle substituent effects upon phosphine variation.

Highlights:

1. New dinitrosyl iron complexes with phosphine ligands have been prepared.
2. X-ray crystallography reveals essentially linear FeNO linkages in these compounds.
3. Phosphine substitutions have effects on the spectroscopy and electrochemistry.
4. Infrared spectroelectrochemistry reveals metal-centered oxidations.

REVISED Ms. Submitted to *J. Organomet. Chem.* 12.12.2013

**Synthesis, Characterization, and Fiber-optic Infrared Reflectance  
Spectroelectrochemical Studies of Some Dinitrosyl Iron Diphosphine  
Complexes  $\text{Fe}(\text{NO})_2\text{L}_2$  ( $\text{L} = \text{P}(\text{C}_6\text{H}_4\text{X})_3$ )**

Myron W. Jones,<sup>a,b\*</sup> Douglas R. Powell,<sup>a</sup> and George B. Richter-Addo<sup>a\*</sup>

<sup>a</sup> *Department of Chemistry and Biochemistry, University of Oklahoma, 101 Stephenson Parkway,  
Norman, OK 73019. Email: grichteraddo@ou.edu*

<sup>b</sup> *Department of Chemistry, Southern Illinois University Edwardsville, IL 62026. Email:  
myrjone@siue.edu.*

---

**ABSTRACT:** A series of iron dinitrosyl complexes of the form  $\text{Fe}(\text{NO})_2(\text{P}(\text{C}_6\text{H}_4\text{X})_3)_2$  ( $\text{X} = p$ -OMe (**1**),  $p$ -Me (**2**),  $m$ -Me (**3**),  $p$ -H (**4**),  $p$ -F (**5**),  $p$ -Cl (**6**),  $p$ -CF<sub>3</sub> (**7**)) has been prepared from the reactions of  $\text{Fe}(\text{NO})_2(\text{CO})_2$  and the respective triarylphosphines. Complexes **1-7** have been characterized by IR and <sup>31</sup>P NMR spectroscopy, and by X-ray crystallography for **1** and **7**. In general, the compounds with the more basic phosphines display lower  $\nu_{\text{NO}}$  stretches in the IR spectra than those with the less basic phosphines, and the trends in  $\nu_{\text{NO}}$  as a function of Hammett parameter and solvent donor/acceptor number was analyzed. The redox behavior of compounds **1-7** in  $\text{CH}_2\text{Cl}_2$  were studied by cyclic voltammetry at a Pt electrode. In general, the compounds undergo one-electron oxidations. Infrared spectroelectrochemistry revealed that the oxidations generate the derivatives with  $\nu_{\text{NOS}}$  that are  $\sim 100 \text{ cm}^{-1}$  higher in energy indicative of  $\text{Fe}(\text{NO})_2$ -centered oxidations.

*Keywords:* iron, nitrosyl, nitric oxide, X-ray, spectroelectrochemistry

## 1. Introduction

Iron is a major target for nitric oxide (NO) in biological systems and in the environment. The resulting ground-state Fe–N–O moiety may be linear or bent [1]. The dinitrosyl Fe(NO)<sub>2</sub> moiety has been suggested as a biologically relevant entity [2-7]. Exogenous and endogenous NO, upon exposure to and contact with Fe-containing biomolecules, generates a species exhibiting a strong EPR signal at  $g = 2.03$  attributed to an “Fe(NO)<sub>2</sub>”-containing species [3]. Other ligands (L) coordinate to the Fe(NO)<sub>2</sub> unit to give Fe(NO)<sub>2</sub>L<sub>x</sub> derivatives [1]; these latter species are collectively referred to as “dinitrosyl iron compounds” (DNICs). DNICs, although mostly discussed in the literature in the realm of biology, also have significance in catalysis as described below. Their syntheses and characterization, to a large extent, preceded their discovery in biology.

Synthetic DNICs display a variety of chemical properties including the ability to transfer oxygen atoms from molecular oxygen to phosphines or alkenes [8-17]. For example, Postel and co-workers demonstrated that the dinitrosyl compounds [Fe(NO)<sub>2</sub>X]<sub>2</sub> (X = Cl, I) react with oxygen in the presence of PPh<sub>3</sub> or OPPh<sub>3</sub> to produce nitrato complexes such as Fe(NO<sub>3</sub>)<sub>2</sub>X(OPPh<sub>3</sub>)<sub>2</sub> [8-12]. These latter nitrato complexes transfer oxygen atoms to phosphines or cyclohexene and regenerate the nitrosyl moiety [10][12].

In 1965, Maxfield reported in a patent the use of dinitrosyl iron halides as effective catalysts for the dimerization of diolefins in the presence of reducing agents [17]. Others later demonstrated that some synthetic DNICs could be used for the cyclodimerization of diolefins when reduced electrochemically [15]. Candlin [13] reported the dimerization of butadiene and isoprene by Fe(NO)<sub>2</sub>(CO)<sub>2</sub>, and Gadd [14] proposed that the photocatalytic dimerization might occur via Fe(NO)<sub>2</sub>(η<sup>2</sup>-C<sub>4</sub>H<sub>6</sub>)(η<sup>4</sup>-C<sub>4</sub>H<sub>6</sub>) as an intermediate. In 1994, Li [18] reported

$\text{Fe}(\text{NO})_2\text{PPh}_3(\eta^2\text{-TCNE})$  as the first stable compound containing an olefin  $\pi$ -bonded to an iron dinitrosyl group.

Returning to the biological significance of DNICs, it was originally proposed that DNICs formed from the reaction of NO with the active center of iron sulfur proteins [19-21]. Recently, Ricci and co-workers reported the crystal structure of a stable complex of human glutathione transferase P1-1 containing a post-translationally modified dinitrosyliron glutathionyl moiety [22]. It is now generally accepted that the iron in biological  $\text{Fe}(\text{NO})_2$  DNICs comes predominately from “freely chelatable iron storage units” and not necessarily from FeS proteins [23-25]. For example, Lancaster et al. recently published work describing the direct reaction of NO with the intercellular labile iron and found that NO rapidly and quantitatively reacts with the iron to form stable DNICs detectable by EPR [24].

All DNICs derive their basic functionality from the dinitrosyl  $\text{Fe}(\text{NO})_2$  moiety. It is known that the carbonyl ligands of  $\text{Fe}(\text{NO})_2(\text{CO})_2$  can be replaced with  $\sigma$  donor ligands (L, L') to yield dinitrosyl complexes of the form  $\text{Fe}(\text{NO})_2\text{L}_2$  or  $\text{Fe}(\text{NO})_2\text{L}'\text{L}$  [1, 26, 27]. Although many such complexes are known, it is somewhat surprising that only a handful of mono-phosphine  $\text{Fe}(\text{NO})_2(\text{CO})(\text{phosphine})$  [26-29] and diphosphine  $\text{Fe}(\text{NO})_2(\text{phosphine})_2$  [8, 26, 29-35] compounds have been reported. In order to determine how the spectroscopic and electrochemical properties of the  $\text{Fe}(\text{NO})_2$  group are affected by small changes on the periphery of some diphosphine complexes, we have prepared and characterized a homologous series of  $\text{Fe}(\text{NO})_2(\text{PAr}_3)_2$  complexes (Ar = aryl group; allowing for a systematic variation in Ar) by FTIR and  $^{31}\text{P}$  NMR spectroscopy, X-ray crystallography, cyclic voltammetry and fiber-optic IR spectroelectrochemistry.

## 2. Experimental

### 2.1 General

All reactions were performed under an atmosphere of pre-purified nitrogen using standard Schlenk glassware and/or in a Labmaster 100 inert atmosphere glove box (Innovative Technology, Inc. Newburyport, MA). Unless otherwise indicated, all experiments were carried out at ambient room temperature.

### 2.2 Chemicals

Solvents were distilled under nitrogen from appropriate drying agents (CaH<sub>2</sub> or Na) or collected under nitrogen from a Pure Solv 400-5-MD Solvent Purification System (Innovative Technology). Fe(NO)<sub>2</sub>(CO)<sub>2</sub> was prepared using a published method developed by Hieber and Beutner, as described by King [36]. Tris(*p*-methoxyphenyl)phosphine (98%), tri-*p*-tolylphosphine (98%), tri-*m*-tolylphosphine (98%), tri(*p*-chlorophenyl)phosphine (99%), and tris(*p*-fluorophenyl)phosphine (99%), were purchased from Strem Chemical Company (Newburyport, MA). Iron pentacarbonyl, triphenylphosphine, (99%), tris(*p*-trifluoromethylphenyl)phosphine (97%) and tetrabutylammonium hexafluorophosphate (98%) were purchased from Sigma-Aldrich Chemical Company (Milwaukee, WI). Chloroform-*d* (99.8%) was purchased from Cambridge Isotope Laboratories (Andover, MA) in single-use ampoules and used as received or drawn from a stock reagent bottle and subjected to at least three freeze-pump-thaw cycles and stored over Grade 514 Type 4A molecular sieves.

### 2.3 Instrumentation

Infrared spectra were recorded using a Bio-Rad FTS 155 FT-IR spectrometer. <sup>31</sup>P{<sup>1</sup>H} NMR spectra were recorded using a Varian Mercury-VX 300 MHz spectrometer equipped with a

four-nuclei autoswitchable pulsed field gradient probe. All chemical shifts ( $\delta$ , ppm) are reported relative to 85%  $\text{H}_3\text{PO}_4$  as an external reference standard ( $\delta = 0$  ppm).

Cyclic voltammograms were recorded using a BAS CV-50W Voltammetric Analyzer (Bioanalytical Systems, West Lafayette, IN) equipped with a three-electrode cell (3 mm Pt disk working electrode, Pt wire auxiliary electrode and a Ag/AgCl or Ag wire quasi-reference electrode). Solutions were 1 mM in analyte and 0.1 M in  $[\text{NBu}_4][\text{PF}_6]$  in  $\text{CH}_2\text{Cl}_2$ . Ferrocene ( $(\eta^5\text{-C}_5\text{H}_5)_2\text{Fe}$ ; Fc) or decamethylferrocene ( $(\eta^5\text{-C}_5\text{Me}_5)_2\text{Fe}$ ) ( $\text{Fc}^*$ ;  $E^{\circ'} = -0.55$  V vs.  $\text{Fc}/\text{Fc}^+$ ) were used as internal reference standards. All potentials (V) are reported relative to the  $\text{Fc}/\text{Fc}^+$  couple.

IR spectroelectrochemical measurements were recorded using a Bruker Vector 22 FT-IR spectrometer equipped with a Remspec mid-IR fiber-optic dip probe and a liquid nitrogen cooled MCT detector (Remspec Corporation, Charlton City, MA). The stainless steel mirror on the liquid transmission head of the fiber-optic dip probe was replaced with a 3 mm Pt disk working electrode and equipped with a custom-made electrochemical cell including a Pt wire auxiliary electrode and a Ag/AgCl or Ag wire quasi-reference electrode as described previously [37].

#### 2.4 Synthesis

Each of the dinitrosyl iron diphosphine complexes was prepared using a method based on slightly modified literature procedures [33, 38]. To the best of our knowledge, only  $\text{Fe}(\text{NO})_2(\text{PPh}_3)_2$  (compound **4**) [34, 35, 38] from this series has been reported prior to our entry in this area. The reactions can be readily monitored by IR spectroscopy and/or  $^{31}\text{P}$  NMR spectroscopy. For example, the reactions were considered complete when the  $^{31}\text{P}$  NMR spectra indicated the generation of a single  $^{31}\text{P}$  NMR peak assigned to the desired products. At the conclusion of each preparative reaction, the complexes were isolated by solvent removal *in vacuo* and purified by dissolution in  $\text{CH}_2\text{Cl}_2$  or  $\text{CHCl}_3$  followed by filtration through Celite®.

Small amounts of pentane or hexane were added to the filtrates, and the products were allowed to recrystallize by slow solvent evaporation under nitrogen.

*Fe(NO)<sub>2</sub>(P(C<sub>6</sub>H<sub>4</sub>-*p*-OCH<sub>3</sub>)<sub>3</sub>)<sub>2</sub>* (**1**): Dark red Fe(NO)<sub>2</sub>(CO)<sub>2</sub> (20 μL, 0.18 mmol) was added by syringe to a toluene solution (5 mL) of P(C<sub>6</sub>H<sub>4</sub>-*p*-OCH<sub>3</sub>)<sub>3</sub> (0.129 g, 0.37 mmol) in a Schlenk tube. The light red solution was stirred, heated and allowed to reflux under nitrogen over a period of 3 h. The solution changed from light red to black/dark brown within the first 20 min. The reaction was monitored by IR spectroscopy and stopped when the IR spectrum indicated the absence of characteristic carbonyl stretching frequencies for Fe(NO)<sub>2</sub>(CO)<sub>2</sub> ( $\nu_{\text{CO}} = 2090 \text{ cm}^{-1}$  and  $2040 \text{ cm}^{-1}$ ) and for the expected mono-carbonyl species ( $\nu_{\text{CO}} = 2002 \text{ cm}^{-1}$ ). Isolated yield: 27%. IR (toluene,  $\text{cm}^{-1}$ ):  $\nu_{\text{NO}} = 1711 \text{ s}$  and  $1667 \text{ s}$ ; also  $1306 \text{ w}$ ,  $1287 \text{ s}$ ,  $1255 \text{ s}$ ,  $1184 \text{ w}$ ,  $1097 \text{ w}$ ,  $826 \text{ w}$ ,  $798 \text{ w}$ .  $^{31}\text{P}\{^1\text{H}\}$  NMR (CDCl<sub>3</sub>):  $\delta$  56.4 (s).

The other complexes were prepared similarly.

*Fe(NO)<sub>2</sub>(P(C<sub>6</sub>H<sub>4</sub>-*p*-CH<sub>3</sub>)<sub>3</sub>)<sub>2</sub>* (**2**): Reaction time = 3 h. Isolated yield: 31%. IR (toluene,  $\text{cm}^{-1}$ ):  $\nu_{\text{NO}} = 1714 \text{ s}$  and  $1670 \text{ s}$ ; also  $1197 \text{ w}$ ,  $1189 \text{ w}$ ,  $1116 \text{ w}$ ,  $1095 \text{ w}$ ,  $806 \text{ s}$ .  $^{31}\text{P}\{^1\text{H}\}$  NMR (CDCl<sub>3</sub>):  $\delta$  58.4 (s).

*Fe(NO)<sub>2</sub>(P(C<sub>6</sub>H<sub>4</sub>-*m*-CH<sub>3</sub>)<sub>3</sub>)<sub>2</sub>* (**3**): Reaction time = 5 h. Isolated yield: 23%. IR (toluene,  $\text{cm}^{-1}$ ):  $\nu_{\text{NO}} = 1715 \text{ s}$  and  $1671 \text{ s}$ ; also  $779 \text{ m}$ ,  $588 \text{ w}$ ,  $549 \text{ w}$ .  $^{31}\text{P}\{^1\text{H}\}$  NMR (CDCl<sub>3</sub>):  $\delta$  60.9 (s).

*Fe(NO)<sub>2</sub>(PPh<sub>3</sub>)<sub>2</sub>* (**4**): The known Fe(NO)<sub>2</sub>(PPh<sub>3</sub>)<sub>2</sub> was prepared using a modified literature method [38]. A toluene solution (5 mL) of P(C<sub>6</sub>H<sub>5</sub>)<sub>3</sub> (94 mg, 0.36 mmol) was treated with Fe(NO)<sub>2</sub>(CO)<sub>2</sub> (20 μL, 0.18 mmol) under nitrogen. The mixture was heated and allowed to reflux over a period of ~3 h. The reaction was monitored by IR spectroscopy and stopped once Fe(NO)<sub>2</sub>(CO)<sub>2</sub> ( $\nu_{\text{CO}} = 2090 \text{ cm}^{-1}$  and  $2040 \text{ cm}^{-1}$ ) or the known Fe(NO)<sub>2</sub>(PPh<sub>3</sub>)(CO) ( $\nu_{\text{CO}} = 2005$

$\text{cm}^{-1}$ ) were no longer detected. Isolated yield: 22%. IR (toluene,  $\text{cm}^{-1}$ ):  $\nu_{\text{NO}} = 1719 \text{ s}$  and  $1678 \text{ s}$ ; also  $1203 \text{ m}$ ,  $1119 \text{ m}$ ,  $543 \text{ m}$ .  $^{31}\text{P}\{^1\text{H}\}$  NMR ( $\text{CDCl}_3$ ):  $\delta 60.9 \text{ (s)}$ .

$\text{Fe}(\text{NO})_2(\text{P}(\text{C}_6\text{H}_4\text{-}p\text{-}\text{F})_3)_2$  (**5**): Reaction time = 3 h. Isolated yield: 23%. IR (toluene,  $\text{cm}^{-1}$ ):  $\nu_{\text{NO}} = 1720 \text{ s}$  and  $1682 \text{ s}$ ; also  $1589 \text{ w}$ ,  $1300 \text{ w}$ ,  $1234 \text{ s}$ ,  $1161 \text{ m}$ ,  $1094 \text{ w}$ ,  $1013 \text{ w}$ ,  $828 \text{ s}$ .  $^{31}\text{P}\{^1\text{H}\}$  NMR ( $\text{CDCl}_3$ ):  $\delta 59.3 \text{ (s)}$ .

$\text{Fe}(\text{NO})_2(\text{P}(\text{C}_6\text{H}_4\text{-}p\text{-}\text{Cl})_3)_2$  (**6**): Reaction time = 3.5 h. Isolated yield: 33%. IR (toluene,  $\text{cm}^{-1}$ ):  $\nu_{\text{NO}} = 1722 \text{ s}$  and  $1682 \text{ s}$ ; also  $1099 \text{ w}$ ,  $1012 \text{ m}$   $818 \text{ m}$ .  $^{31}\text{P}\{^1\text{H}\}$  NMR ( $\text{CDCl}_3$ ):  $\delta 60.9 \text{ (s)}$ .

$\text{Fe}(\text{NO})_2(\text{P}(\text{C}_6\text{H}_4\text{-}p\text{-}\text{CF}_3)_3)_2$  (**7**): Reaction time = 3.5 h. Isolated yield: 33%. IR (toluene,  $\text{cm}^{-1}$ ):  $\nu_{\text{NO}} = 1728 \text{ m}$  and  $1687 \text{ s}$ ; also  $1397 \text{ w}$ ,  $1321 \text{ m}$ ,  $1281 \text{ w}$ ,  $1185 \text{ w}$ ,  $1169 \text{ m}$ ,  $1129 \text{ m}$ ,  $1062 \text{ w}$ ,  $1015 \text{ w}$ ,  $832 \text{ m}$ .  $^{31}\text{P}\{^1\text{H}\}$  NMR ( $\text{CDCl}_3$ ):  $\delta 63.8 \text{ (s)}$ .

## 2.5 X-ray Crystallography

Suitable crystals for the structural analyses of compounds **1** and **7** were grown by slow evaporation of solvent under nitrogen at ambient room temperature. All samples were mounted on the end of a plastic loop using an inert oil (Paratone N). The samples were cooled to  $100(2) \text{ K}$  and maintained at this temperature throughout the duration of the data collection. Intensity data for each compound were collected using a diffractometer equipped with a Bruker APEX ccd area detector and graphite-monochromated Mo  $\text{K}\alpha$  radiation ( $\lambda = 0.71073 \text{ \AA}$ ). The structures were solved by direct methods using the SHELXTL software package (Version 6.10) and refined by full-matrix least-squares methods on  $F^2$ . All non-hydrogen atoms were refined anisotropically and all hydrogen atoms were included using idealized parameters.

Crystallographic collection and refinement parameters for the  $\text{Fe}(\text{NO})_2(\text{PAR}_3)_2$  crystals are given in Table 1.

### 2.5.1 $Fe(NO)_2(P(C_6H_4-p-OCH_3)_3)_2$ (**1**)

A red plate-shaped crystal of dimensions 0.50 x 0.31 x 0.08 mm was selected for structural analysis. Cell parameters were determined from a non-linear least squares fit of 6550 peaks in the range  $2.34 < \theta < 27.91^\circ$ . A total of 29988 reflections were measured in the range  $2.02 < \theta < 26.00^\circ$  using  $\omega$  oscillation frames. The data were corrected for absorption by a semi-empirical method giving minimum and maximum transmission factors of 0.774 and 0.962. The data were merged to form a set of 7618 independent data with  $R(int) = 0.0353$  and a coverage of 99.6 %. The monoclinic space group  $P2_1/c$  was determined by systematic absences and statistical tests and verified by subsequent refinement.

One of the *p*-methoxyphenyl groups of one of the phosphines was disordered; restraints on the positional parameters of the disordered atoms were required. The occupancies of these disordered groups refined to 0.521(3) and 0.479(3).

### 2.5.2 $Fe(NO)_2(P(C_6H_4-p-CF_3)_3)_2$ (**7**)

A red prism-shaped crystal of dimensions 0.33 x 0.25 x 0.15 mm was selected for structural analysis. Cell parameters were determined from a non-linear least squares fit of 9530 peaks in the range  $2.29 < \theta < 28.26^\circ$ . A total of 22582 reflections were measured in the range  $1.61 < \theta < 26.00^\circ$  using  $\omega$  oscillation frames. The data were corrected for absorption by a semi-empirical method giving minimum and maximum transmission factors of 0.843 and 0.928. The data were merged to form a set of 8855 independent data with  $R(int) = 0.0183$  and a coverage of 99.1 %. The triclinic space group  $P\bar{1}$  was determined by statistical tests and verified by subsequent refinement. The structure included one *n*-pentane solvent molecule (not shown). The *n*-pentane was best modeled using the *SQUEEZE* program [39].

CCDC 959031 (**1**) and CCDC 959032 (**7**) contain the supplementary crystallographic data. These data can be obtained free of charge from The Cambridge Crystallographic Data Center via <http://www.ccdc.cam.ac.uk/conts/retrieving.html>. The crystal structures of **2** [40], **5** [41], and **6** [42] have been published separately.

**Table 1.** Crystallographic collection and refinement parameters for the Fe(NO)<sub>2</sub>(PAr<sub>3</sub>)<sub>2</sub> products.

Complex	<b>1</b>	<b>7</b> •(C <sub>5</sub> H <sub>12</sub> )
Empirical formula	C <sub>42</sub> H <sub>42</sub> FeN <sub>2</sub> O <sub>8</sub> P <sub>2</sub>	C <sub>47</sub> H <sub>36</sub> F <sub>18</sub> FeN <sub>2</sub> O <sub>2</sub> P <sub>2</sub>
Formula weight	820.57	1120.57
Crystal system	Monoclinic	Triclinic
Space group	<i>P2</i> <sub>1</sub> / <i>c</i>	<i>P</i> $\bar{1}$
Unit cell dimensions		
<i>a</i> (Å)	14.467(4)	10.933(2)
<i>b</i> (Å)	10.936(4)	13.024(2)
<i>c</i> (Å)	24.848(8)	16.851(3)
$\alpha$ (°)	90	103.280(5)
$\beta$ (°)	98.498(8)	101.957(5)
$\gamma$ (°)	90	92.653(6)
Volume (Å <sup>3</sup> )	3888(2)	2273.5(7)
<i>Z</i> , <i>Z'</i>	4, 1	2, 1
Density (calculated) Mg/m <sup>3</sup>	1.402	1.637
Wavelength (Å)	0.71073	0.71073
<i>F</i> (000)	1712	1132
Absorption coefficient (mm <sup>-1</sup> )	0.527	0.519
Max. and min. transmission	0.962 and 0.774	0.928 and 0.843
Theta range for data collection (°)	2.02 to 26.00	1.61 to 26.00
Reflections collected	29988	22582
Independent reflections	7618 [R(int) = 0.0353]	8855 [R(int) = 0.0183]
Data/restraints/parameters	7618/141/569	8855/0/604
<i>wR</i> ( <i>F</i> <sup>2</sup> all data) <sup>a</sup>	<i>wR</i> 2 = 0.1136	<i>wR</i> 2 = 0.1031
<i>R</i> ( <i>F</i> obsd data) <sup>b</sup>	<i>R</i> 1 = 0.0420	<i>R</i> 1 = 0.0380
Goodness-of-fit on <i>F</i> <sup>2</sup>	1.038	1.004
Observed data [ <i>I</i> > 2σ( <i>I</i> )]	6330	8196
Largest and mean shift / s.u.	0.000 and 0.000	0.001 and 0.000
Largest diff. peak and hole (e/Å <sup>3</sup> )	0.494 and -0.348	1.116 and -0.434

$$^a wR2 = \{ \sum [w(F_o^2 - F_c^2)^2] / \sum [w(F_o^2)^2] \}^{1/2} \quad ^b R1 = \sum ||F_o| - |F_c|| / \sum |F_o|$$

### 3. Results

#### 3.1 Synthesis

The  $\text{Fe}(\text{NO})_2(\text{PAr}_3)_2$  compounds were prepared in refluxing toluene using a modified literature procedure as depicted in Figure 1 [33, 38].

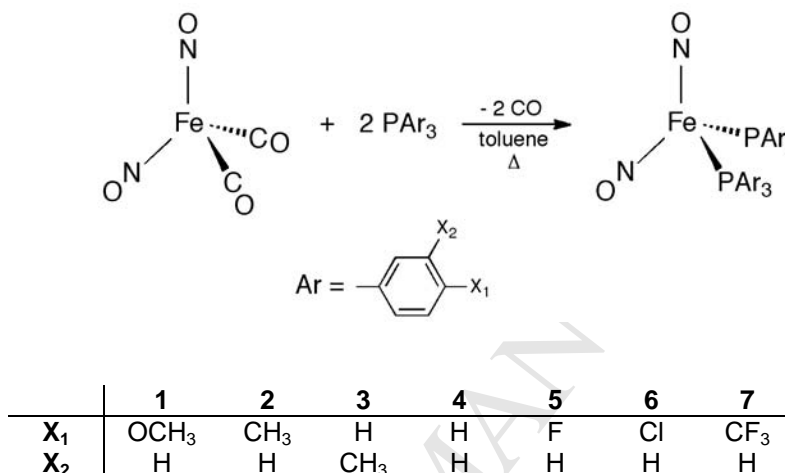


**Figure 1.** Reaction scheme depicting the formation of the  $\text{Fe}(\text{NO})_2(\text{PAr}_3)_2$  products.

The compounds were isolated in 22–27% non-optimized yields as brown (**1–3** and **6**) black (**4–5**), or red-brown (**7**) solids. Of the compounds in this series, only the parent compound **4**, and a brief mention of **2** [43], had been reported previously [29, 34, 35, 38], although the related  $\text{Fe}(\text{NO})_2(\text{PR}_3)_2$  ( $\text{PR}_3 =$  phosphine or phosphite) [32, 33, 35] and  $\text{Fe}(\text{NO})_2(\text{P–P})$  ( $\text{P–P} =$  chelating/bidentate phosphine) [8, 26, 30, 31, 33, 34] compounds are known. The solids appear to be stable under nitrogen in for more than twelve months as determined by IR spectroscopy and/or cyclic voltammetry.

#### 3.2 IR Spectroscopy

The progress of the reactions to prepare the  $\text{Fe}(\text{NO})_2(\text{PAr}_3)_2$  compounds were monitored by IR spectroscopy. The solution IR spectrum of the starting compound  $\text{Fe}(\text{NO})_2(\text{CO})_2$  is shown

in Figure 2a, and exhibits two carbonyl and two nitrosyl signals; each pair of bands correspond to the symmetric and antisymmetric stretches of the dicarbonyl and dinitrosyl moieties [1].

The carbonyl stretching vibrations ( $\nu_{\text{CO}} = 2087 \text{ cm}^{-1}$  and  $2036 \text{ cm}^{-1}$ ) appear at higher energy than the nitrosyl stretches ( $\nu_{\text{NO}} = 1807 \text{ cm}^{-1}$  and  $1760 \text{ cm}^{-1}$ ) and the symmetric stretch of each pair appears at higher energy than the antisymmetric stretch.

Addition of the respective phosphine to a stirred toluene solution of  $\text{Fe}(\text{NO})_2(\text{CO})_2$  at room temperature under nitrogen resulted in the replacement of at least one carbonyl group as indicated by the disappearance of the associated IR bands of the starting compound. For example, the IR spectrum of the reaction mixture containing  $\text{Fe}(\text{NO})_2(\text{CO})_2$  and  $\text{P}(\text{C}_6\text{H}_4\text{-}p\text{-F})_3$  before heating to full reflux is shown in Figure 2b. The spectrum indicates that a mixture of the mono and disubstituted products forms prior to reflux. In addition to the bands assigned to the dinitrosyl group of the product  $\text{Fe}(\text{NO})_2(\text{P}(\text{C}_6\text{H}_4\text{-}p\text{-F})_3)_2$  at  $1720 \text{ cm}^{-1}$  and  $1682 \text{ cm}^{-1}$ , the band at  $2009 \text{ cm}^{-1}$  is assigned to the carbonyl group of  $\text{Fe}(\text{NO})_2(\text{P}(\text{C}_6\text{H}_4\text{-}p\text{-F})_3)(\text{CO})$  intermediate, and the bands at  $1763 \text{ cm}^{-1}$  and  $1720 \text{ cm}^{-1}$  are assigned to the dinitrosyl group of this intermediate. All the bands are shifted to lower frequencies than those present in  $\text{Fe}(\text{NO})_2(\text{CO})_2$ , as shown for other monosubstitution reactions with other phosphines [27, 28].

The remaining carbonyl group in  $\text{Fe}(\text{NO})_2(\text{P}(\text{C}_6\text{H}_4\text{-}p\text{-F})_3)(\text{CO})$  was completely replaced upon the application of heat; the IR spectrum for the product,  $\text{Fe}(\text{NO})_2(\text{P}(\text{C}_6\text{H}_4\text{-}p\text{-F})_3)_2$  is shown in Figure 2c. As with the replacement of one carbonyl from  $\text{Fe}(\text{NO})_2(\text{CO})_2$ , replacement of the carbonyl from  $\text{Fe}(\text{NO})_2(\text{P}(\text{C}_6\text{H}_4\text{-}p\text{-F})_3)(\text{CO})$  was accompanied with a decrease in the IR stretching frequencies for the dinitrosyl group. The dinitrosyl stretching frequencies,  $\nu_{\text{NOs}}$ , in  $\text{Fe}(\text{NO})_2(\text{P}(\text{C}_6\text{H}_4\text{-}p\text{-F})_3)_2$  are lower relative to the  $\nu_{\text{NOs}}$  present in both  $\text{Fe}(\text{NO})_2(\text{CO})_2$  and

$\text{Fe}(\text{NO})_2(\text{P}(\text{C}_6\text{H}_4\text{-}p\text{-F})_3)(\text{CO})$ . The IR spectral shifts for the reactions between  $\text{Fe}(\text{NO})_2(\text{CO})_2$  and the other phosphines at room temperature were similar.

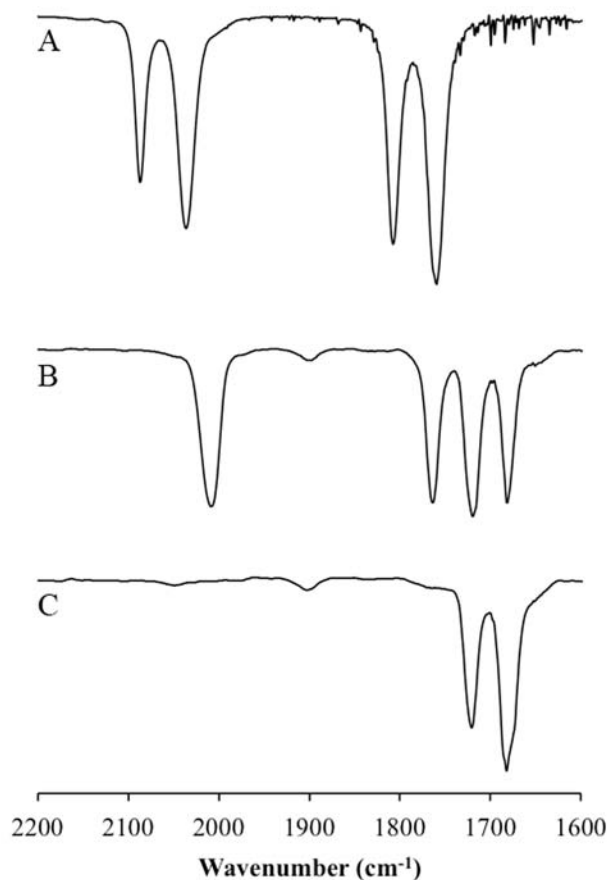


**Figure 2.** IR spectra of (A)  $\text{Fe}(\text{NO})_2(\text{CO})_2$  in  $\text{CH}_2\text{Cl}_2$ ;  $\nu_{\text{CO}}$  (sym) =  $2087\text{ cm}^{-1}$ ,  $\nu_{\text{CO}}$  (asym) =  $2036\text{ cm}^{-1}$ ;  $\nu_{\text{NO}}$  (sym) =  $1807\text{ cm}^{-1}$ ,  $\nu_{\text{NO}}$  (asym) =  $1760\text{ cm}^{-1}$ . (B) the reaction mixture during the preparation of  $\text{Fe}(\text{NO})_2(\text{P}(\text{C}_6\text{H}_4\text{-}p\text{-F})_3)_2$  in toluene prior to full reflux, showing the presence of a mixture of the mono-substituted intermediate  $\text{Fe}(\text{NO})_2(\text{P}(\text{C}_6\text{H}_4\text{-}p\text{-F})_3)(\text{CO})$  ( $\nu_{\text{CO}} = 2009\text{ cm}^{-1}$ ,  $\nu_{\text{NO}} = 1763\text{ cm}^{-1}$  and  $1720\text{ cm}^{-1}$ ) and the desired product  $\text{Fe}(\text{NO})_2(\text{P}(\text{C}_6\text{H}_4\text{-}p\text{-F})_3)_2$  ( $\nu_{\text{NO}} = 1720\text{ cm}^{-1}$  and  $1682\text{ cm}^{-1}$ ), and (C) the reaction mixture during the preparation of  $\text{Fe}(\text{NO})_2(\text{P}(\text{C}_6\text{H}_4\text{-}p\text{-F})_3)_2$  in toluene after several hours of reflux.

In all cases, it was necessary to carry out the reaction at refluxing toluene temperature ( $\sim 80\text{ }^\circ\text{C}$ ) to affect complete replacement of the second carbonyl. This observation is consistent with previous studies on other dinitrosyl iron complexes [18, 27, 38].

The IR data for each complex in three different solvents are summarized in Table 2. The  $\nu_{\text{NOS}}$  for compounds containing electron-donating substituents were lower than those for compounds containing electron-withdrawing substituents. A solvent effect was observed on the  $\nu_{\text{NOS}}$ . In general, the  $\nu_{\text{NOS}}$  obtained in  $\text{CH}_2\text{Cl}_2$  were between those determined in toluene and in acetonitrile. These results will be discussed later.

### 3.3 $^{31}\text{P}$ NMR Spectroscopy

Proton decoupled  $^{31}\text{P}$  NMR spectra were obtained at room temperature in  $\text{CDCl}_3$ . The chemical shifts for each compound along with the chemical shifts for the corresponding free ligands are shown in Table 2. Each compound exhibited a single resonance consistent with two chemically equivalent phosphorus atoms in the 56–64 ppm range (vs. 85%  $\text{H}_3\text{PO}_4$  as an external reference standard), and the complexed P signals were shifted ~70 ppm from those of the free ligands [26, 30, 31]. In general, the compounds with electron-withdrawing substituents had higher chemical shifts ( $\delta$ ) appearing further upfield from the parent compound (*p*-H) while, in contrast, compounds with electron-donating substituents had lower chemical shifts appearing farther downfield from the parent compound. There seems to be some inconsistencies in this trend, however, and this will be addressed later.

**Table 2.** IR and  $^{31}\text{P}\{^1\text{H}\}$  NMR spectroscopic data for the  $\text{Fe}(\text{NO})_2(\text{PAr}_3)_2$  products.<sup>a</sup>

Complex	Substituent	$\sigma^a$	$\text{p}K_a^b$	$\nu_{\text{NO}} (\text{cm}^{-1})$			$\delta$ (ppm) <sup>c</sup>		$\Delta\delta$
				$\text{CH}_3\text{CN}$	$\text{CH}_2\text{Cl}_2$	toluene	free ligand	complex	
<b>1</b>	<i>p</i> -OCH <sub>3</sub>	−0.27	4.57	1703	1704	1711	−9.6	56.4	66.0
				1660	1659	1667			
<b>2</b>	<i>p</i> -CH <sub>3</sub>	−0.17	3.84	1708	1708	1714	−7.4	58.4	65.8
				1665	1663	1670			
<b>3</b>	<i>m</i> -CH <sub>3</sub>	−0.07	3.30	1710	1711	1715	−4.7	60.9	65.6
				1667	1664	1671			
<b>4</b>	<i>p</i> -H	0.00	2.73	1712	1715	1719	−4.9	60.9	65.8
				1670	1670	1678			
<b>5</b>	<i>p</i> -F	0.06	1.97	1715	1719	1720	−8.6	59.3	67.9
				1673	1674	1682			
<b>6</b>	<i>p</i> -Cl	0.23	1.03	1720	1723	1722	−8.0	60.9	68.9
				1677	1678	1682			
<b>7</b>	<i>p</i> -CF <sub>3</sub>	0.54	−1.55	1728	1730	1728	−5.5	63.8	69.3
				1686	1685	1687			

<sup>a</sup>  $\sigma$  = the Hammett  $\sigma_p$  or  $\sigma_m$  substituent parameter. <sup>b</sup> The cited  $\text{p}K_a$  corresponds to the acid dissociation process:  $\text{H}(\text{PAr}_3)^+ \rightleftharpoons \text{H}^+ + \text{PAr}_3$ . The  $\text{p}K_a$  data was obtained from the literature [44, 45]. <sup>c</sup> Chemical shifts,  $\delta$  (ppm), are referenced to 85%  $\text{H}_3\text{PO}_4$  set as  $\delta = 0$  ppm.

### 3.4 X-ray crystallography

Despite the intense research efforts by many research groups into the chemistry and relevance of DNICs, it is surprising that very little structural data was available on the dinitrosyl bisphosphine  $\text{Fe}(\text{NO})_2(\text{PAr}_3)_2$  compounds prior to our work in this area [8, 29, 30]. Suitable crystals for X-ray diffraction studies were grown by slow evaporation of solvent under nitrogen at ambient room temperature. Molecular structures for compounds **1** and **7** are shown in Figures 3 and 4, respectively. Selected bond distances ( $\text{\AA}$ ) and angles ( $^\circ$ ) for **1** and **7** are presented in Table 3, and compared with our recently published data for compounds **2** [40], **5** [41], and **6** [42].

**Table 3.** Selected bond lengths (Å) and angles (°) for the Fe(NO)<sub>2</sub>(PAr<sub>3</sub>)<sub>2</sub> products.

Complex	Fe–N	N–O	Fe–P	∠P–Fe–P	∠N–Fe–N	∠O••Fe••O	∠Fe–N–O
<b>1</b>	1.655(2)	1.200(3)	2.254(1)	105.97(3)	128.49(11)	127.96	177.65(19)
	1.654(2)	1.184(3)	2.247(1)				177.5(2)
<b>2</b> [40]	1.655(2)	1.191(2)	2.260(1)	106.00(2)	129.89(7)	130.31	179.31(16)
	1.659(2)	1.195(2)	2.240(1)				175.05(15)
<b>3</b> [40]	1.651(2)	1.190(2)	2.257(1)	105.57(2)	124.29(8)	121.67	179.10(16)
	1.652(2)	1.187(2)	2.245(1)				173.84(15)
<b>4</b> [29]	1.650(7)	1.190(10)	2.267(2)	111.9(1)	123.8(4)	122.47	178.2(7)
		1.190(10)					178.2(7)
<b>5</b> [41]	1.657(2)	1.191(3)	2.242(1)	108.27(4)	127.02(11)	125.62	178.1(2)
	1.653(2)	1.197(3)	2.247(1)				177.0(2)
<b>6</b> [42]	1.659(2)	1.188(2)	2.241(1)	106.80(3)	127.78(7)	127.15	178.76(15)
	1.658(2)	1.186(2)	2.231(1)				177.67(14)
<b>7</b>	1.655(2)	1.184(2)	2.248(1)	105.25(2)	122.20(9)	118.46	175.96(18)
	1.657(2)	1.185(2)	2.250(1)				173.50(17)

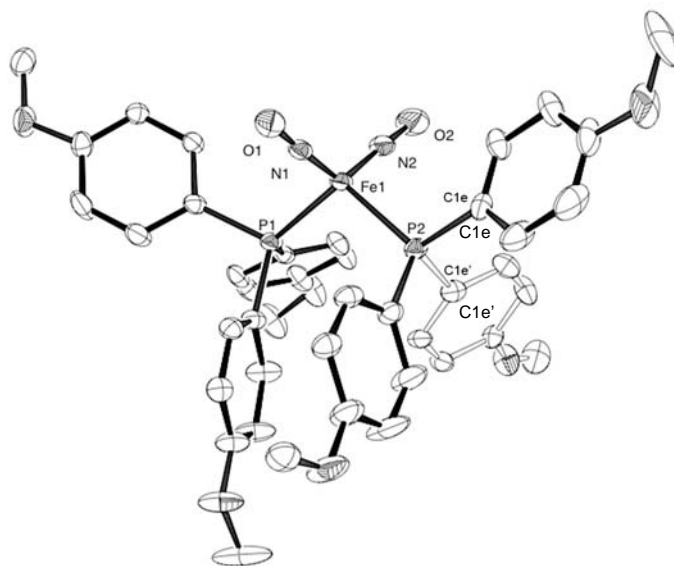


**Figure 3.** Molecular structure of **1**,  $\text{Fe}(\text{NO})_2(\text{P}(\text{C}_6\text{H}_4\text{-}p\text{-OCH}_3)_3)_2$ . Hydrogen atoms have been omitted for clarity. The figure depicts the disorder of one of the phenyl rings of one of the phosphine ligands. The displacement ellipsoids are drawn at the 50% probability level.

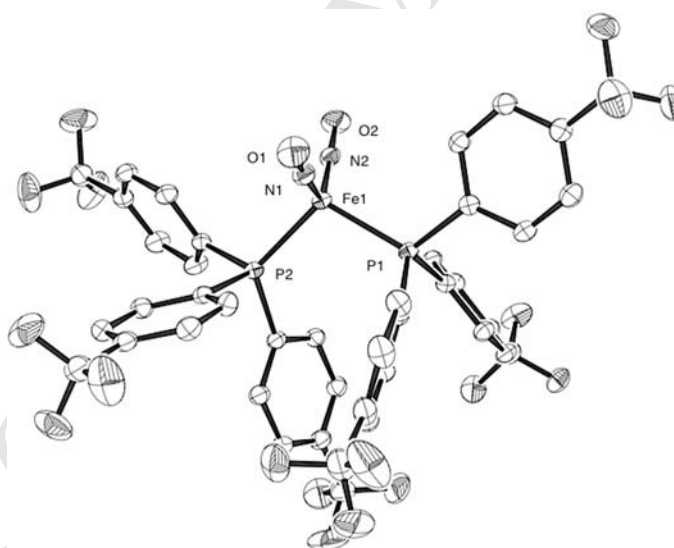


**Figure 4.** Molecular structure of **7**,  $\text{Fe}(\text{NO})_2(\text{P}(\text{C}_6\text{H}_4\text{-}p\text{-CF}_3)_3)_2$ . Hydrogen atoms have been omitted for clarity. The displacement ellipsoids are drawn at the 50% probability level.

### 3.5 Electrochemistry

The redox behavior of compounds **1–7** were examined in CH<sub>2</sub>Cl<sub>2</sub> using cyclic voltammetry. Each compound undergoes a 1-electron oxidation process within the solvent potential range examined under the experimental conditions described in the Experimental section. No reduction processes were observed. The cyclic voltammogram for **5**, Fe(NO)<sub>2</sub>(P(C<sub>6</sub>H<sub>4</sub>-*p*-F)<sub>3</sub>)<sub>2</sub>, is shown in Figure 5.

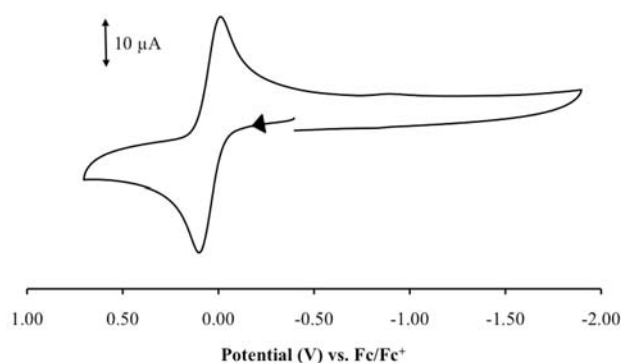


**Figure 5.** Cyclic voltammogram for a 1 mM solution of Fe(NO)<sub>2</sub>(P(C<sub>6</sub>H<sub>4</sub>-*p*-F)<sub>3</sub>)<sub>2</sub> (**5**) in CH<sub>2</sub>Cl<sub>2</sub> containing 0.1 M NBu<sub>4</sub>PF<sub>6</sub> at a scan rate of 200 mV s<sup>-1</sup>.

The cyclic voltammograms for compounds **1–3** (*p*-OCH<sub>3</sub>, *p*-CH<sub>3</sub>, and *m*-CH<sub>3</sub>) and **5–6** (*p*-F and *p*-Cl) were similar to that of **4** (*p*-H) except that the formal electrode potential,  $E^{\circ'}$  =  $[(E_{pa} + E_{pc})/2]$ , was shifted more negative for **1–3** and more positive for **5–6** relative to that of **4**. The  $E_{pa}$  for **7**, Fe(NO)<sub>2</sub>(P(C<sub>6</sub>H<sub>4</sub>-*p*-CF<sub>3</sub>)<sub>3</sub>)<sub>2</sub>, was the most positive of the seven compounds studied and its cyclic voltammogram was significantly different from those of the other six compounds. A representative cyclic voltammogram for **7** is shown in Figure 6.

The electrochemical data for each compound is summarized in Table 4. Compounds containing electron-donating substituents had lower formal electrode potentials,  $E^{\circ'}$ , while

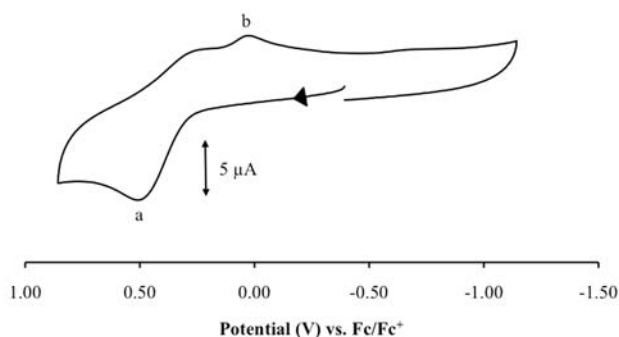


**Figure 6.** Cyclic voltammogram for a 1 mM solution of  $\text{Fe}(\text{NO})_2(\text{P}(\text{C}_6\text{H}_4\text{-}p\text{-CF}_3)_2)$  (**7**) in  $\text{CH}_2\text{Cl}_2$  containing 0.1 M  $\text{NBu}_4\text{PF}_6$  at  $200 \text{ mV s}^{-1}$ .

**Table 4.** Formal electrode potentials (V vs  $\text{Fc}/\text{Fc}^+$ ) and related electrochemical data for the  $\text{Fe}(\text{NO})_2(\text{PAR}_3)_2$  products in  $\text{CH}_2\text{Cl}_2$  (scan rate =  $0.1 \text{ V s}^{-1}$ ).<sup>a</sup>

Complex	Substituent	$\sigma^b$	$E_{\text{pa}}^c$	$E_{\text{pc}}^c$	$\Delta E_{\text{p}}^d$	$E^{\circ\prime e}$	$i_{\text{pc}}/i_{\text{pa}}^f$	$\Delta E_{\text{p(ref)}}^g$
<b>1</b>	<i>p</i> -OCH <sub>3</sub>	-0.27	-0.15	-0.27	0.12	-0.21	1.0	0.09
<b>2</b>	<i>p</i> -CH <sub>3</sub>	-0.17	-0.12	-0.26	0.14	-0.19	0.97	0.11
<b>3</b>	<i>m</i> -CH <sub>3</sub>	-0.07	-0.11	-0.21	0.10	-0.16	0.89	0.08
<b>4</b>	<i>p</i> -H	0.00	-0.08	-0.17	0.09	-0.13	1.0	0.08
<b>5</b>	<i>p</i> -F	0.06	0.10	0.00	0.10	0.05	1.0	0.09
<b>6</b>	<i>p</i> -Cl	0.23	0.14	0.06	0.08	0.10	1.0	0.06
<b>7</b>	<i>p</i> -CF <sub>3</sub>	0.54	0.51	--	--	--	--	0.06

<sup>a</sup> All potentials are referenced to the  $\text{Fc}/\text{Fc}^+$  couple. <sup>b</sup>  $\sigma$  = the Hammett substituent parameter. <sup>c</sup>  $E_{\text{pa}}$  and  $E_{\text{pc}}$  = the anodic and cathodic peak potentials, respectively. <sup>d</sup>  $\Delta E_{\text{p}} = |E_{\text{pa}} - E_{\text{pc}}|$ . <sup>e</sup>  $E^{\circ\prime}$  is the formal electrode potential =  $(E_{\text{pa}} + E_{\text{pc}})/2$ . <sup>f</sup>  $i_{\text{pc}}/i_{\text{pa}}$  represents the ratio of peak currents defined by  $(i_{\text{pc}})_0/i_{\text{pa}} + (0.485(i_{\text{sp}})_0)/i_{\text{pa}} + 0.086$ . <sup>g</sup>  $\Delta E_{\text{p(ref)}} = \Delta E_{\text{p}}$  of the internal reference standard;

those with electron-withdrawing substituents had higher formal electrode potentials. The cyclic voltammetry results obtained for **1** and **7** will now be described as representative examples and compared to the other compounds.

The cyclic voltammogram of  $\text{Fe}(\text{NO})_2(\text{P}(\text{C}_6\text{H}_4\text{-}p\text{-OCH}_3)_3)_2$  (**1**) in  $\text{CH}_2\text{Cl}_2$  exhibits a reversible one-electron oxidation at  $E^{\circ'} = -0.21$  V vs.  $\text{Fc}/\text{Fc}^+$  at a scan rate ( $\nu$ ) of  $100 \text{ mV s}^{-1}$ . The separation in peak potentials ( $\Delta E_p$ ) is 120 mV; this  $\Delta E_p$  increases slightly with increasing scan rate, being in one determination 98 mV at  $0.10 \text{ V s}^{-1}$  and 134 mV at  $0.50 \text{ V s}^{-1}$ . Under the same conditions, the ferrocene internal reference standard has a  $\Delta E_p$  of 76 mV at  $0.10 \text{ V s}^{-1}$  and 97 mV at  $0.50 \text{ V s}^{-1}$ . The anodic to cathodic peak current ratio ( $i_{pc}/i_{pa}$ ) is 1.0, and remained constant over the  $0.05\text{--}1.2 \text{ V s}^{-1}$  range. The  $i_{pa}$  value varies linearly with  $\nu^{1/2}$  over the entire scan rate range employed indicative of a diffusion controlled electrooxidation. Lastly, in the case of  $\text{Fe}(\text{NO})_2(\text{P}(\text{C}_6\text{H}_4\text{-}p\text{-OCH}_3)_3)_2$ , there was some evidence for a second oxidation when the scan was extended to the solvent limit; however, this feature could not be fully characterized using our solvent system.

As mentioned previously the cyclic voltammogram of compound **7** is significantly different from the other six compounds. The cyclic voltammogram of **7** in  $\text{CH}_2\text{Cl}_2$  exhibits a chemically irreversible oxidation. At a scan rate of  $200 \text{ mV s}^{-1}$  the anodic peak potential occurs at  $E_{pa} = 0.51$  V vs.  $\text{Fc}/\text{Fc}^+$  (feature *a* in Figure 6). A small cathodic peak occurs at  $E_{pc} = -0.04$  V vs.  $\text{Fc}/\text{Fc}^+$ . This peak (feature *b* in Figure 6) appears larger if the scan is taken farther in the anodic direction (i.e. closer to the solvent limit), and the  $i_{pa}$  value varies linearly with  $\nu^{1/2}$  over the entire scan rate range employed.

### 2.3.6 Infrared Spectroelectrochemistry

The IR spectroelectrochemistry of each compound (**1–7**) was examined at room temperature in CH<sub>2</sub>Cl<sub>2</sub>. The applied potential  $E_{\text{appl}}$  was typically set at 50–120 mV more positive than  $E_{\text{pa}}$ , and the data obtained are summarized in Table 5. Each of the electrogenerated compounds exhibited symmetric and antisymmetric nitrosyl stretching frequencies that were ~100 cm<sup>-1</sup> higher than the  $\nu_{\text{NOS}}$  observed in the neutral compounds. Not surprisingly, the  $\nu_{\text{NOS}}$  for compounds containing electron-donating substituents were lower than those for compounds containing electron-withdrawing substituents.

**Table 5.** IR spectroelectrochemical data obtained for the Fe(NO)<sub>2</sub>(PAR<sub>3</sub>)<sub>2</sub> products in CH<sub>2</sub>Cl<sub>2</sub>.<sup>a</sup>

Complex	$E_{\text{appl}}$	$\nu_{\text{NO}}$ (cm <sup>-1</sup> )		
		Neutral	Oxidized	$\Delta\nu_{\text{NO}}$
<b>1</b>	-0.05	1704	1805	101
		1659	1758	99
<b>2</b>	-0.06	1708	1810	102
		1663	1763	100
<b>3</b>	0.01	1711	1812	101
		1664	1764	100
<b>4</b>	0.04	1715	1816	101
		1670	1767	97
<b>5</b>	0.17	1719	1820	101
		1674	1770	96
<b>6</b>	0.26	1723	1823	100
		1678	1772	94
<b>7</b>	0.62	1730	1827	97
		1685	1759,1778	74

<sup>a</sup>  $E_{\text{appl}}$  is the applied potential (V) relative to the ferrocene-ferrocenium couple, Fc/Fc<sup>+</sup>.  $E_{\text{appl}}$  was typically set at 0.05–0.12 V more positive than  $E_{\text{pa}}$ .  $\Delta\nu_{\text{NO}}$  is the difference between  $\nu_{\text{NO}}$  for the singly oxidized compound and the corresponding  $\nu_{\text{NO}}$  for the neutral compound.

A representative IR difference spectrum recorded during controlled potential oxidation of Fe(NO)<sub>2</sub>(P(C<sub>6</sub>H<sub>4</sub>-*p*-F)<sub>3</sub>)<sub>2</sub> is shown at the top of Figure 7. The  $\nu_{\text{NOS}}$  for the neutral starting

compound are shown as disappearing at  $1674\text{ cm}^{-1}$  and  $1719\text{ cm}^{-1}$ . The  $\nu_{\text{NOS}}$  for the oxidized species appear at  $1770\text{ cm}^{-1}$  and  $1820\text{ cm}^{-1}$  which suggests the formation of a cationic  $\text{Fe}(\text{NO})_2$  containing species such as  $[\text{Fe}(\text{NO})_2(\text{P}(\text{C}_6\text{H}_4\text{-}p\text{-}\text{F})_2)]^+$ .

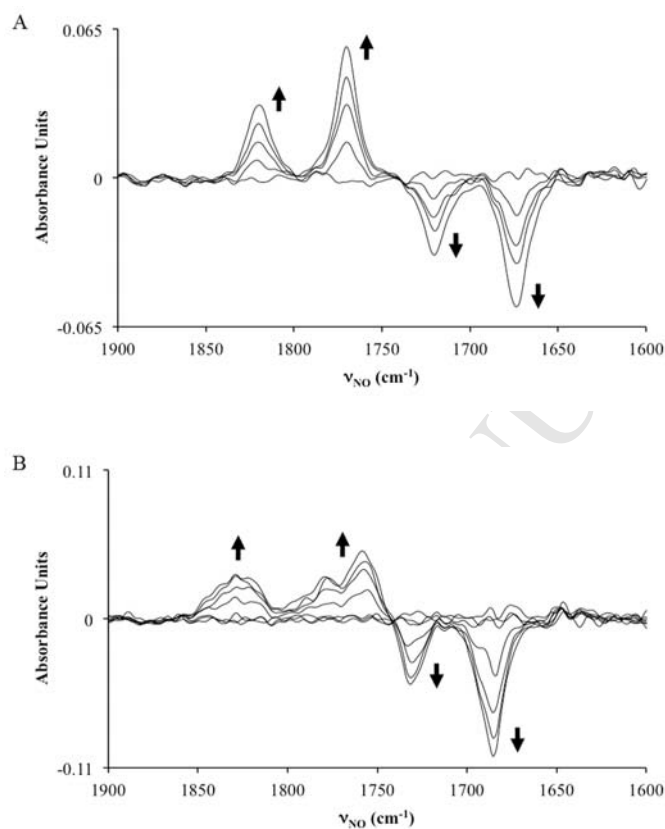


**Figure 7.** (A) IR difference spectrum recorded during the oxidation of **5**,  $\text{Fe}(\text{NO})_2(\text{P}(\text{C}_6\text{H}_4\text{-}p\text{-}\text{F})_3)_2$ , in  $\text{CH}_2\text{Cl}_2$  containing  $0.1\text{ M}$   $[\text{NBu}_4][\text{PF}_6]$  at  $E_{\text{appl}} = 0.17\text{ V}$  vs.  $\text{Fc}/\text{Fc}^+$ .  $\nu_{\text{NOS}}$  for the neutral compound are shown growing downward at  $1674\text{ cm}^{-1}$  and  $1719\text{ cm}^{-1}$  while  $\nu_{\text{NOS}}$  for the oxidized species appear growing upward at  $1770\text{ cm}^{-1}$  and  $1820\text{ cm}^{-1}$ . (B) IR difference spectrum recorded during the oxidation of **7**,  $\text{Fe}(\text{NO})_2(\text{P}(\text{C}_6\text{H}_4\text{-}p\text{-}\text{CF}_3)_3)_2$ , in  $\text{CH}_2\text{Cl}_2$  containing  $0.1\text{ M}$   $[\text{NBu}_4][\text{PF}_6]$  at  $E_{\text{appl}} = 0.62\text{ V}$  vs.  $\text{Fc}/\text{Fc}^+$ .  $\nu_{\text{NOS}}$  for the neutral compound are shown growing downward at  $1685\text{ cm}^{-1}$  and  $1730\text{ cm}^{-1}$  while evidence of the  $\nu_{\text{NOS}}$  for the oxidized species appear growing upward at  $1759\text{ cm}^{-1}$ ,  $1778\text{ cm}^{-1}$  and  $1827\text{ cm}^{-1}$ .

The difference spectra for the other compounds studied were all similar to that obtained for **5** except for the spectrum recorded during the oxidation of **7** which is depicted at the bottom of Figure 7. The peaks for the oxidized species in the spectrum for **7** are not as clearly defined as those for the other compounds, which suggests that the formation of the presumed cationic

Fe(NO)<sub>2</sub> containing species may convert to other species under our spectroelectrochemical conditions.

## 4. Discussion

### 4.1 Synthesis

The starting compound, Fe(NO)<sub>2</sub>(CO)<sub>2</sub>, is a toxic, air sensitive, deep red liquid at room temperature (m.pt. 18 °C) [36]. Previous preparations of Fe(NO)<sub>2</sub>L<sub>2</sub> (L = σ donor ligand) compounds have involved carrying out the reaction directly with Fe(NO)<sub>2</sub>(CO)<sub>2</sub> or from [Fe(NO)<sub>2</sub>(μ-X)]<sub>2</sub> (X = Cl, Br, I) under reducing conditions [26, 31, 33, 34, 38, 46, 47]. These types of compounds have also been prepared by a reductive substitution reaction involving [(RS)<sub>2</sub>Fe(NO)<sub>2</sub>]<sup>-</sup> anions with excess PPh<sub>3</sub> or by reaction of phosphines with Fe(NO)<sub>2</sub>(PR<sub>3</sub>)X [35, 48]. Bitterwolf published a one-pot synthesis of Fe(NO)<sub>2</sub>(PAR<sub>3</sub>)<sub>2</sub> type compounds based on the reductive substitution of Na<sub>2</sub>[Fe<sub>2</sub>(NO)<sub>4</sub>(μ-S<sub>2</sub>O<sub>3</sub>)<sub>2</sub>] in the presence of phosphines and phosphites [32].

The current preparation of Fe(NO)<sub>2</sub>(PAR<sub>3</sub>)<sub>2</sub> type compounds is based on a modified literature procedure involving the reaction of Fe(NO)<sub>2</sub>(CO)<sub>2</sub> with substituted triarylphosphines in toluene [33, 38]. Toluene was selected because it had a boiling point high enough to allow displacement of the second carbonyl ligand under refluxing conditions.

## 4.2 Infrared Spectroscopy

It is known that the substituents on the phenyl rings of triarylphosphines affect their basicities [44, 49-51]. The position of the dinitrosyl stretching frequency measured upon coordination with a phosphine ligand is related to the electron donor capacity or the Lewis basicity of the ligand and to the donor or acceptor capacity of the solvent in which the measurement is taken [52-55]. Several methods have been used to quantify this type of substituent effect. One of the most widely applied and useful tools is the Hammett substituent constant or Hammett parameter  $\sigma$  [56].

Hammett parameters are linear free energy relationships that can be used as a measure of the electronic effects of ligands [57, 58]. Hammett constants for each substituent used in this work and the corresponding  $pK_a$ s of the protonated phosphine ligands are given in Table 2; the Hammett parameter,  $\sigma$ , correlates linearly with the  $pK_a$ s of the phosphines used in this study [44, 45]. The order of ligand basicity is the same as the order of the Hammett  $\sigma_p$  and  $\sigma_m$  parameters (i.e., Hammett constants for substituents in *para* and *meta* positions). We thus set out to determine if a correlation exists between  $\sigma$  and the spectroscopic properties of the  $Fe(NO)_2(PAr_3)_2$  products.

A plot showing the IR stretching frequencies for each substituted compound in three different solvents (toluene,  $CH_2Cl_2$  and acetonitrile) as a function of Hammett parameter is shown in Figure 8. Separate plots of the IR stretching frequencies for the dinitrosyl groups as a function of Hammett parameter in the same three solvents are shown in Figure 9.

In general, compounds with the more basic phosphines have lower  $\nu_{NOS}$  while compounds with the less basic phosphines have higher  $\nu_{NOS}$ . The effect of solvent appears to be greater on the symmetric  $\nu_{NOS}$  of compounds with electron-donating substituents. The  $\nu_{NOS}$  of

the compound with the most electron-withdrawing substituent, **7** (*p*-CF<sub>3</sub>) appear to not be as affected by solvent differences as those with more electron donating substituents. For most of the series, frequencies obtained in the non-polar and non-coordinating solvent toluene were higher than those obtained in CH<sub>2</sub>Cl<sub>2</sub> (a polar non-coordinating solvent) or in acetonitrile (a polar coordinating solvent). The  $\nu_{\text{NOS}}$  obtained in CH<sub>2</sub>Cl<sub>2</sub> were generally in-between those obtained in toluene and in acetonitrile although they tended to be closer to those obtained in acetonitrile as can be seen in Figure 8. The effect of solvent on  $\nu_{\text{NO}}$  appears to be greater on the compounds with the more basic ligands.

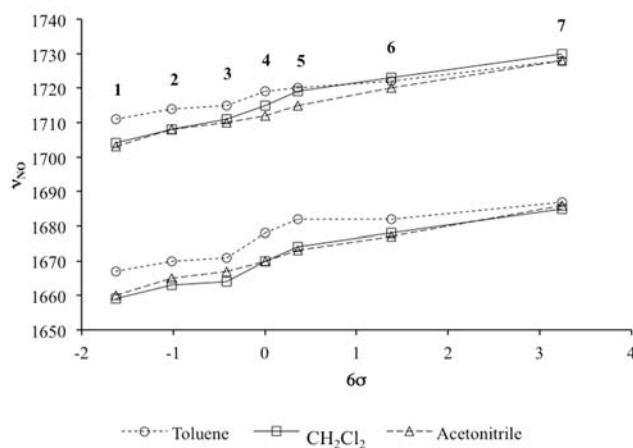


**Figure 8.** Plot depicting the symmetric and antisymmetric  $\nu_{\text{NOS}}$  in toluene, CH<sub>2</sub>Cl<sub>2</sub> and acetonitrile versus the Hammett substituent parameter.

In Figures 8 and 9 it can be observed that electron-withdrawing substituents on the triarylphosphines, PAr<sub>3</sub>, shifted the  $\nu_{\text{NOS}}$  to higher frequencies (by 9–16 cm<sup>-1</sup>) relative to the parent compound Fe(NO)<sub>2</sub>(PPh<sub>3</sub>)<sub>2</sub> (i.e. *p*-H). In contrast, electron-donating substituents shifted  $\nu_{\text{NOS}}$  to lower frequencies. (by 8–11 cm<sup>-1</sup>). The largest shifts in  $\nu_{\text{NO}}$  were observed in the polar CH<sub>2</sub>Cl<sub>2</sub> and the polar coordinating solvent acetonitrile.

The shifts in  $\nu_{\text{NO}}$  as a function of Hammett parameter can be rationalized on the basis of the ligand basicity and the concept of backbonding. The more basic ligands (those with electron-donating substituents) contribute more electron density to the iron center and thus increase backbonding from the filled  $d$ -orbitals on the metal to the antibonding  $\pi^*$  orbitals on the nitrosyls resulting in relatively lower  $\nu_{\text{NO}}$ s. Conversely, the less basic ligands (those with electron-withdrawing substituents) contribute less electron density to the iron center and, as a result, the metal to ligand backbonding is less as indicated by relatively higher  $\nu_{\text{NO}}$ s.

While the plots for toluene and  $\text{CH}_2\text{Cl}_2$  fit linearly with the Hammett parameter, a slight bending can be detected near the point where the substituents change from electron-withdrawing to electron-donating. It is possible for the data to be fitted to two separate lines at this juncture as shown in Figures 9A and B. This observation tends to support having different modes of interaction between the different solvent types and the two classes of  $\text{Fe}(\text{NO})_2(\text{PAr}_3)_2$  compounds. In addition, the two lines *may* also be explained by the  $\text{Fe}(\text{NO})_2$  moiety in the two classes adopting two slightly different conformations (or extent of *atracto* distortions) in different solvent types. Toluene and  $\text{CH}_2\text{Cl}_2$  are both non-coordinating solvents and the plots of  $\nu_{\text{NO}}$  versus  $\sigma$  for both of these solvents possess the two-line feature. Compound **3**,  $\text{Fe}(\text{NO})_2(\text{P}(\text{C}_6\text{H}_4\text{-}m\text{-CH}_3)_3)_2$  deviates from the lines in  $\text{CH}_2\text{Cl}_2$  and in toluene more than any of the *para* substituted compounds. In contrast, the plot of  $\nu_{\text{NO}}$  versus  $\sigma$  for acetonitrile is quite linear and cannot be fitted to two separate lines. This suggests that the coordinating solvent interacts in a way not present in toluene or  $\text{CH}_2\text{Cl}_2$ .

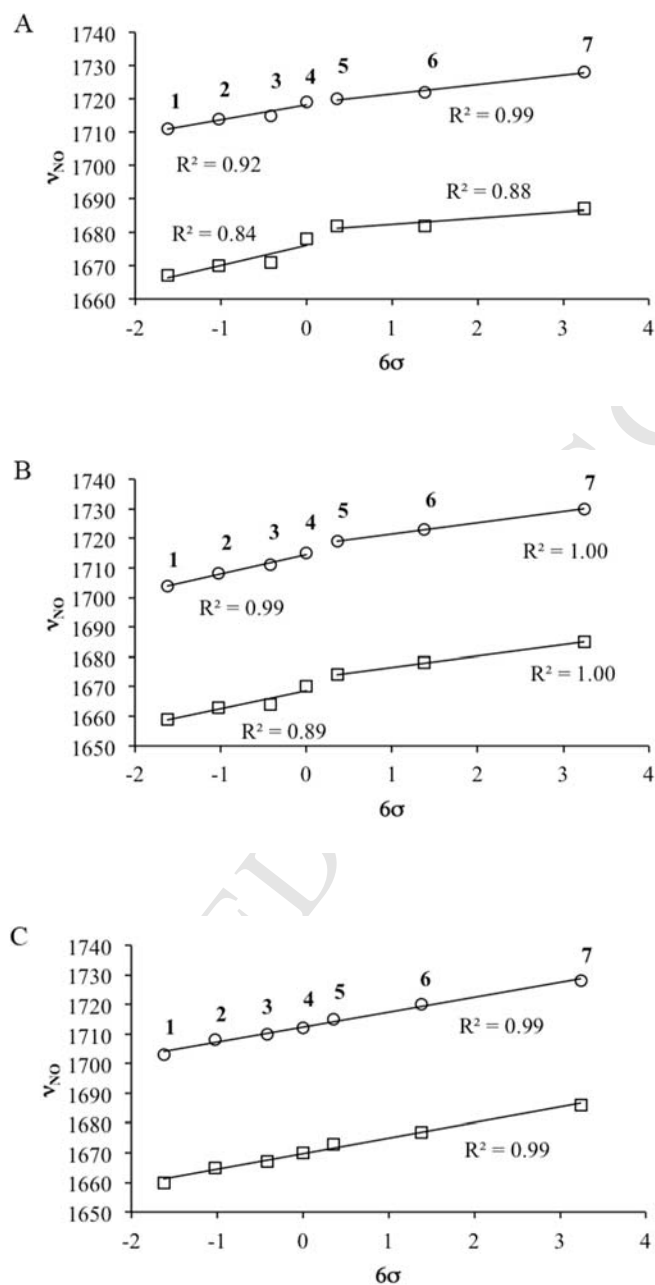


**Figure 9.** Plots depicting the symmetric and antisymmetric  $\nu_{NO}^s$  for  $\text{Fe}(\text{NO})_2(\text{PAr}_3)_2$  compounds in (A) toluene, (B)  $\text{CH}_2\text{Cl}_2$  and (C) acetonitrile vs. the Hammett substituent parameter.

If the oxygen atom on the dinitrosyl complexes acts as a donor to the solvent, there should be a relationship between the IR stretching frequency and the solvent acceptor number

(AN) [59-61]. Similarly, if the solvent behaves as a donor towards the dinitrosyl compounds of interest there should be a relationship between the  $\nu_{\text{NO}}$  and the solvent donor number (DN) [60-62]. The acceptor and donor numbers (AN/DN; in kcal/mol) for the solvents used in this work and for some other representative solvents are: cyclohexane (0/0), ether (3.9/19.2), toluene (8.2/0.1),  $\text{CCl}_4$  (8.6/0), dioxane (10.8/14.8), acetonitrile (18.9/14.1),  $\text{CH}_2\text{Cl}_2$  (20.4/1), and  $\text{CHCl}_3$  (23.1/4) [59, 61, 63, 64].

Plots showing the influence of the solvent acceptor number on  $\nu_{\text{NO}}$  are shown in Figure 10 and plots showing the influence of the solvent donor number on  $\nu_{\text{NO}}$  are shown in Figure 11. From these plots it can be seen that both the donor and acceptor properties of the solvents clearly have an effect on  $\nu_{\text{NO}}$ . As the solvent acceptor number increases  $\nu_{\text{NO}}$  generally decreases. This trend is generally consistent throughout the series. Some small exceptions occur upon going from the polar coordinating acetonitrile solvent to the polar non-coordinating  $\text{CH}_2\text{Cl}_2$ .

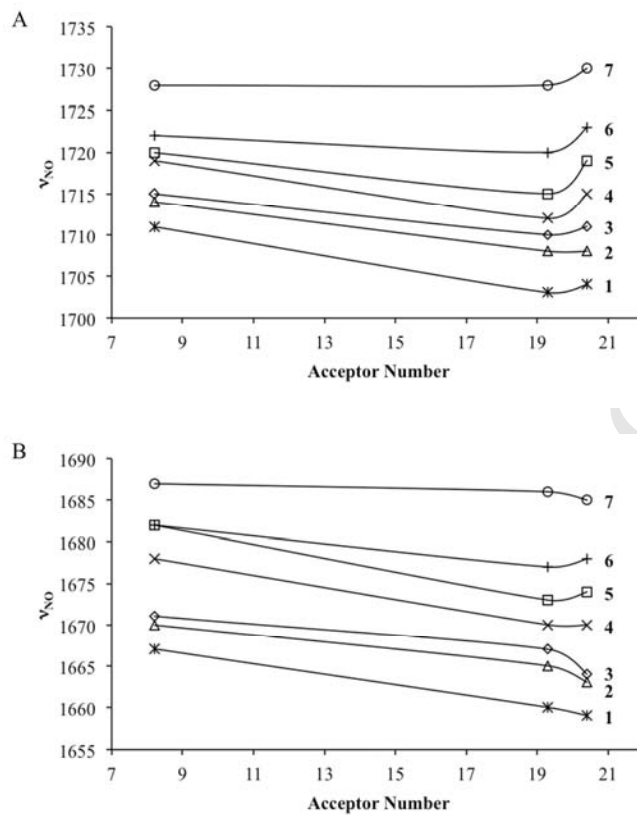


**Figure 10.** Plots depicting (A) the symmetric and (B) the antisymmetric  $\nu_{\text{NO}}$  for each  $\text{Fe}(\text{NO})_2(\text{PAr}_3)_2$  as a function of solvent acceptor number. The solvents are (from left to right) toluene, acetonitrile, and  $\text{CH}_2\text{Cl}_2$ . (AN = 8.2, 18.9 and 20.4 respectively).

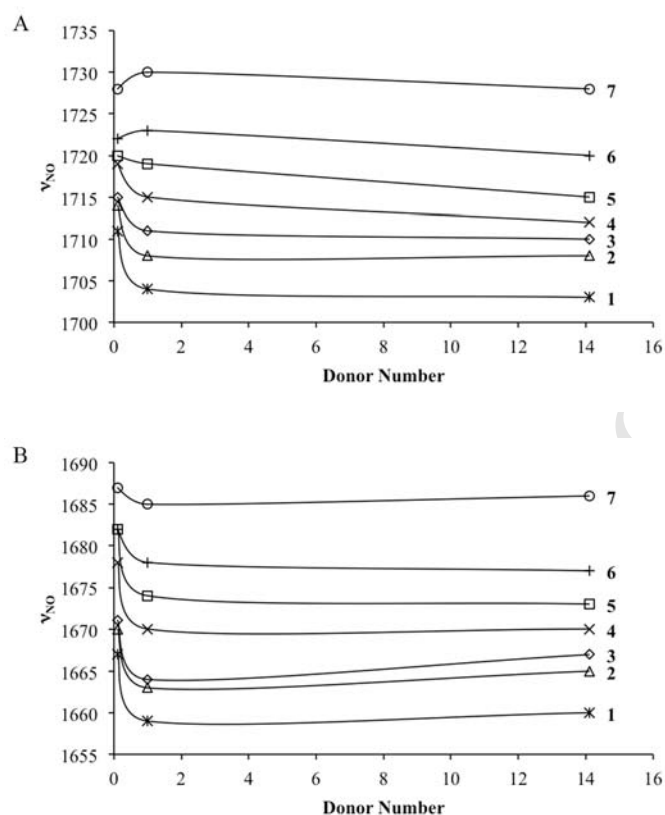


**Figure 11.** Plots depicting (A) the symmetric  $\nu_{\text{NO}}$  and (B) the antisymmetric  $\nu_{\text{NO}}$  for each  $\text{Fe}(\text{NO})_2(\text{PAr}_3)_2$  as a function of solvent donor number. The solvents are (from left to right) toluene,  $\text{CH}_2\text{Cl}_2$  and acetonitrile. (DN = 0.1, 1.0 and 14.1 respectively).

An interesting pattern is also observed when the  $\nu_{\text{NO}}$  data is plotted against the solvent donor number (Figure 11). In general,  $\nu_{\text{NO}}$  decreases with increasing donor number. The effect is much more pronounced upon moving from the less basic phosphines to the more basic phosphines (top-to-bottom in the plots). Two exceptions stand out among the symmetric  $\nu_{\text{NO}}$  data in that the *p*- $\text{CF}_3$  and the *p*-Cl compounds both increase slightly before decreasing.

These solvent acceptor and donor number analyses herein are consistent with the notion that the DNICs studied can behave as both donors toward the solvent and acceptors from the

solvent. The results suggest an interaction between the solvent acceptor orbitals and the *basic* dinitrosyl oxygens. Essentially the NO ligands behave as Lewis bases toward the solvent. However, dinitrosyl moieties are rather complex as there is not a single  $\nu_{\text{NO}}$  trend to follow. In general, as the solvent's ability to accept electron density increases (i.e. increasing AN), we observe lower  $\nu_{\text{NOS}}$ . In a complementary fashion, these results also support the notion that the solvent may donate electron density to the DNICs. As the solvent donor number increased, the  $\nu_{\text{NOS}}$  generally decreased, which is an observation consistent with the fact that increased electron density at the metal results in enhanced metal to ligand backdonation of electron density. While the donor number results do not show a large steady decrease in  $\nu_{\text{NO}}$  over the entire range studied, there is a clear initial decrease in  $\nu_{\text{NO}}$  upon going from the non-polar and non-coordinating toluene to the more polar solvents. Both the solvent acceptor and the donor number results nicely support some previous related solvent effects studies involving  $\text{Fe}(\text{NO})_2(\text{P}(\text{C}_6\text{H}_5)_3)_2$  and some related DNICs [53].

Gutmann described the variation of  $\nu_{\text{NOS}}$  on complexes of the type  $\text{Fe}(\text{NO})_2(\text{CO})\text{L}$  (where  $\text{L} = \text{CO}, \text{P}(\text{OC}_6\text{H}_5)_3, \text{As}(\text{C}_6\text{H}_5)_3, \text{P}(\text{C}_6\text{H}_5)_3$  and  $\text{P}(\text{C}_6\text{H}_{11})_3$ ) in three different solvents ( $\text{C}_6\text{H}_{12}, \text{CCl}_4$  and  $\text{CHCl}_3$ ) and found that the frequency differences of the iron nitrosyl carbonyl derivatives of the type  $\text{Fe}(\text{NO})_2(\text{CO})\text{L}$  were increased by increased solvent acceptor number and in the order of increasing basicity of the ligand [54]. The results of this current work are consistent with his finding even though our set of ligands are more uniform and the changes between each ligand are relatively small (i.e. the *para* or *meta* substituent) and far removed from the coordination center.

### 4.3 $^{31}\text{P}$ NMR spectroscopy

The  $^{31}\text{P}$  NMR data as a function of the Hammett parameter  $\sigma_p$  can immediately be fitted to two separate lines as shown in Figure 12a. The line on the left (compounds **1**, **2** and **4**) consists of the chemical shifts of compounds with electron-donating substituents on  $\text{PAr}_3$ . A second line on the right (compounds **5**, **6** and **7**) consists of the chemical shifts of compounds with electron-withdrawing substituents on  $\text{PAr}_3$ . Thus, in general, on going from the more basic phosphines to the less basic phosphines the chemical shift appears further upfield. It is not entirely clear why there is a break in the linear trend in  $^{31}\text{P}$  chemical shifts on going from electron-donating substituents to electron-withdrawing substituents. However, the absence of a single linear correlation between the chemical shift and basicity indicates that the inductive effect that controls basicity is not the major influence on the chemical shift in these complexes.

Upon closer inspection of the Hammett plot in Figure 12a it can be seen that it is possible to group the  $^{31}\text{P}$  NMR data in a different way. Some of the substituents contain lone pairs (*p*- $\text{OCH}_3$ , *p*- $\text{F}$ , *p*- $\text{Cl}$ ) and are thus might be able to participate in a direct resonance interaction with the phosphorus atom. Considering only those substituents capable of direct resonance yields a clear linear correlation (Figure 12b). Curiously, the *p*- $\text{CF}_3$  substituent also falls on the trend line.

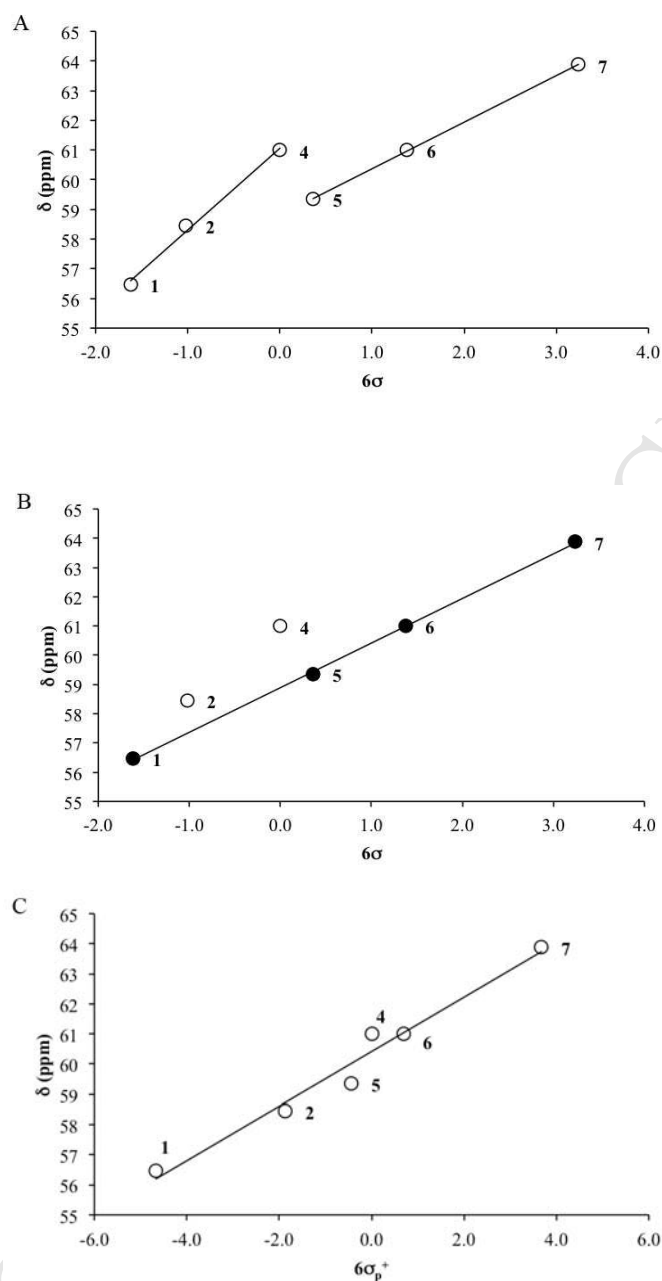


**Figure 12.** (A) Plot depicting the  $\delta(^{31}\text{P})$  chemical shifts for each  $\text{Fe}(\text{NO})_2(\text{PAR}_3)_2$  as a function of the Hammett parameter. (B) an alternative correlation for (A). The dark filled markers indicate those substituents capable of participating in a direct resonance interaction with the phosphorus atom. (C) Plot of the  $\delta(^{31}\text{P})$  chemical shifts as a function of the Brown-Okamoto constant  $\sigma_p^+$ . The Brown-Okamoto constant is used in cases where substituents are capable of participating in a direct resonance interaction with the phosphorus atom.

It is known that the Hammett parameter gives poor correlations when resonance interactions are involved. A separate set of linear free energy relationships (LFER) Hammett

parameters are available for use in cases where resonance interactions are possible. A plot of  $\delta(^{31}\text{P})$  versus the Brown-Okamoto constant  $\sigma_p^+$  [58, 65] gives a straight line as shown in Figure 12c.

It is evident that the  $^{31}\text{P}$  NMR chemical shift is affected by small changes on the periphery of the  $\text{PAr}_3$  ligands. Based on our data, some combination of ligand basicity and resonance factors play important roles. However, the relative contribution of each factor is not clear at this time.

#### 4.4 X-ray Crystallography

As has been discussed in the previous sections, the electron density at the iron atom in  $\text{Fe}(\text{NO})_2(\text{PAr}_3)_2$  compounds is affected by the use of different substituents attached to the aromatic rings of the phosphine ligands. It is reasonable to expect structural differences in the  $\text{Fe}(\text{NO})_2$  fragment as a consequence of different substituents being attached.

All of the compounds studied possess a distorted tetrahedral geometry around at the iron center. The iron is bound to two nitrosyl groups via the nitrogen atoms and to two phosphine ligands via the phosphorus atom. The N–Fe–N bond angles are in the range  $122^\circ$ – $130^\circ$  while the P–Fe–P bond angles are in the range  $105^\circ$ – $109^\circ$ . The Fe–N–O bond angles range between  $173^\circ$ – $180^\circ$ . The Fe–N bond lengths of  $\sim 1.65 \text{ \AA}$  are all shorter than  $1.688(3)$  found in  $\text{Fe}(\text{NO})_2(\text{CO})_2$  [66], but are similar to those of  $\text{Fe}(\text{NO})_2(\text{dppe})$  ( $1.658(5)$  and  $1.651(4) \text{ \AA}$ ) [8] and  $\text{Fe}(\text{NO})_2(\text{PPh}_2\text{FcPPh}_2)$  ( $1.653(6)$ ,  $1.654(5) \text{ \AA}$ ) [30].

The  $\text{Fe}(\text{NO})_2$  units are in “*attracto*” conformations where the  $\text{O}\bullet\bullet\text{Fe}\bullet\bullet\text{O} < \text{N–Fe–N}$  bond angle (Figure 13); similar “*attracto*” conformations have been determined in the crystal

structures of the chelated phosphine complexes  $\text{Fe}(\text{NO})_2(\text{dppe})$  [8] and  $\text{Fe}(\text{NO})_2(\text{PPh}_2\text{FcPPh}_2)$  [30].

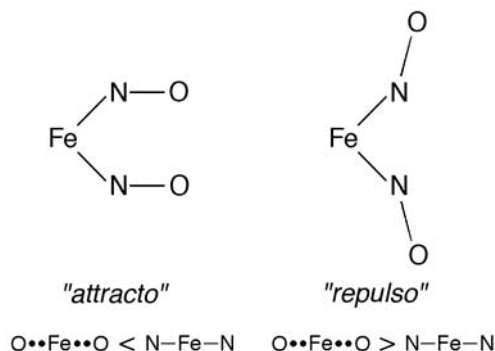


**Figure 13.** Schematic depicting “attracto” and “repulso” conformations of the  $\text{Fe}(\text{NO})_2$  group [1].

There doesn't appear to be a clear trend in the X-ray data of complexes **1-7**, most likely due to the fact that the changes are very small. However, some noteworthy observations can be made by comparing the two extremes (electron-donating substituents vs. electron-withdrawing substituents) relative to the parent  $\text{Fe}(\text{NO})_2(\text{PPh}_3)_2$  compound.

The  $\text{O}\bullet\bullet\text{Fe}\bullet\bullet\text{O}$  bond angle of the parent compound is  $\sim 122.47^\circ$  [29]. Replacement of the hydrogen with the more electron donating *p*-OMe group is accompanied by an *increase* in the  $\text{O}\bullet\bullet\text{Fe}\bullet\bullet\text{O}$  bond angle of  $\sim 5.5^\circ$ . Conversely, replacement of the of the hydrogen with *p*-CF<sub>3</sub>, a more electron withdrawing group is accompanied by a  $\sim 4.0^\circ$  *decrease* in the  $\text{O}\bullet\bullet\text{Fe}\bullet\bullet\text{O}$  bond angle. All three of these phosphines have cone angles of  $\sim 145^\circ$  and thus we would expect sterics to be a minor factor. Similar results are observed within the M–N–O bond angles. Overall, electron-donating substituents on the phosphines promote increased metal-ligand backbonding which is manifested in wider bond angles. The opposite is true for electron withdrawing substituents.

The molecular structures for the neutral 18-electron  $\text{Fe}(\text{NO})_2(\text{PPh}_3)_2$  and the one-electron-oxidized derivative  $[\text{Fe}(\text{NO})_2(\text{PPh}_3)_2]\text{PF}_6$  were published by Albano [29] and Atkinson [33], respectively. Atkinson noted a number of important differences between the structure of the neutral compound and that of the cation. First, oxidation of  $\text{Fe}(\text{NO})_2(\text{PPh}_3)_2$  was accompanied with a substantial increase (0.095 Å) in the Fe–P bond length from 2.267(2) Å in the neutral compound to 2.362(1) Å in the cation. This is an effect that is consistent with increased Fe–P  $\pi$  back-bonding character in the HOMO of  $\text{Fe}(\text{NO})_2(\text{PPh}_3)_2$ . The Fe–N bond was lengthened ( $\Delta +0.011$  Å) from 1.650(7) Å in the neutral compound to 1.661(4) Å in the cation. The effects on these two bonds was consistent with  $\pi$  back-bonding to the nitrosyl  $\pi^*$  orbitals, but this effect was relatively small. Nevertheless, Atkinson reported a higher nitrosyl IR stretching frequency for the cation [ $\Delta\nu_{\text{NO}} = \sim 110 \text{ cm}^{-1}$ ] which is consistent with a 1-electron metal centered oxidation. The geometry around the iron center of  $(\text{Ar}_3\text{P})_2\text{Fe}(\text{NO})_2$  changed markedly upon oxidation. The interphosphine angle, P–Fe–P, *increased* by  $\sim 11^\circ$  and the internitrosyl angle *decreased* by  $\sim 10^\circ$ . Finally, the nitrosyl ligands in the cation bent inward toward each other in an “*attracto*” conformation.

All of the observations reported by Atkinson were consequences of the single-electron oxidation of  $\text{Fe}(\text{NO})_2(\text{PPh}_3)_2$  which is the extreme case of perturbing electron density at the metal center. It might be expected that some intermediate effects would be observed, as described in this work using substituted aryl-phosphine ligands to “fine tune” the density to a lesser extent. The results of electrochemical oxidation of our compounds are discussed in the next section.

#### 4.5 Electrochemistry

The cyclic voltammogram for compound **4**,  $\text{Fe}(\text{NO})_2(\text{P}(\text{C}_6\text{H}_6)_3)_2$ , was previously reported by Atkinson to have a single diffusion controlled fully reversible oxidation in  $\text{CH}_2\text{Cl}_2$  at  $E^{\circ'} = 0.37 \text{ V vs. SCE}$  ( $-0.10 \text{ vs. Fc/Fc}^+$ ). No reductions were observed in the potential range  $0.00$  to  $-1.80 \text{ V vs. SCE}$ . The present determination for **4** agrees within  $30 \text{ mV}$  of Atkinson's result. Except for the compound **7**,  $\text{Fe}(\text{NO})_2(\text{P}(\text{C}_6\text{H}_4\text{-}p\text{-CF}_3)_3)_2$ , each of the other compounds analyzed exhibited a single reversible oxidation within the potential range examined (Table 4).

Changing the basicity of the ligands attached to the iron metal center can be expected to affect the formal redox potential of the compound. Compounds with more electron density available at the metal center should be easier to oxidize relative to the parent compound whereas those compounds with less electron density available should be more difficult to oxidize than the parent. It was observed that compounds with the most basic phosphine ligands were the easiest to oxidize as indicated by their lower  $E^{\circ'}$  values. Changing to more electron withdrawing substituents caused a noticeable increase in  $E^{\circ'}$  from  $-0.21 \text{ V vs. Fc/Fc}^+$  in **1** to  $0.10 \text{ V}$  in **6**, a difference of  $0.31 \text{ V}$ . The largest single  $\Delta E^{\circ'}$  ( $\Delta E^{\circ'} = E_x - E_{\text{parent}}$ ) occurred upon changing from  $p\text{-H}$  to  $p\text{-F}$  ( $\Delta E^{\circ'} = 0.18 \text{ V}$ ). All of the other differences were  $< 0.05 \text{ V}$ .  $E_{\text{pa}}$  for **7**,  $\text{Fe}(\text{NO})_2(\text{P}(\text{C}_6\text{H}_4\text{-}p\text{-CF}_3)_3)_2$ , was much more positive than that of any of the other compounds occurring at  $0.51 \text{ V vs. Fc/Fc}^+$  which is  $0.37 \text{ V}$  more positive than  $E_{\text{pa}}$  in **6**,  $\text{Fe}(\text{NO})_2(\text{P}(\text{C}_6\text{H}_4\text{-}p\text{-Cl})_3)_2$ .

A Hammett plot of  $E^{\circ'}$  versus  $6\sigma$  can be fitted to two lines which look very similar to the two line plot obtained from the  $^{31}\text{P}$  NMR data analysis (Figure 14a). However, in this case, the compounds clearly fall into two separate groups (i.e. electron withdrawing and electron donating).

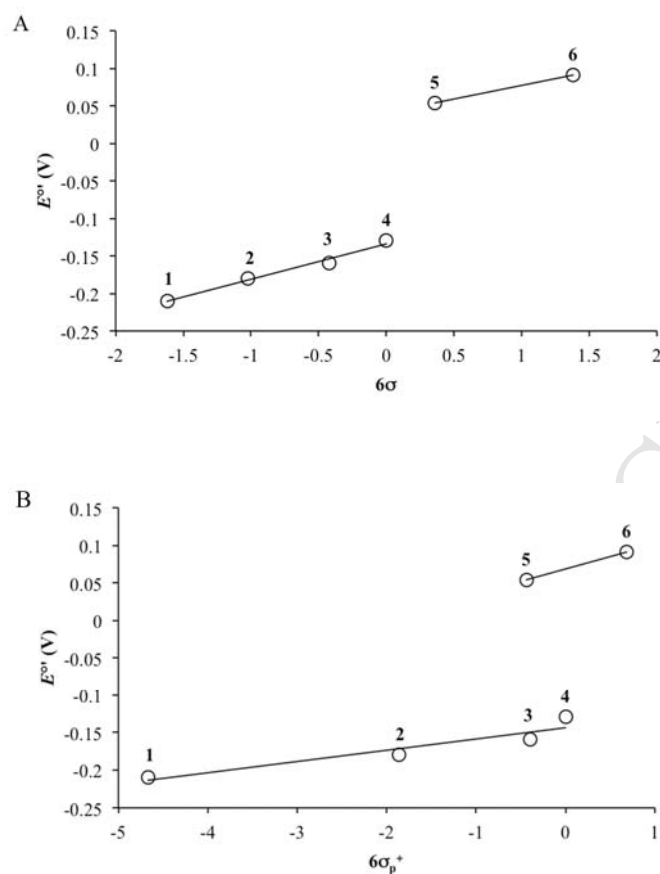


**Figure 14.** Plot depicting  $E^{\circ\prime}$  for each  $\text{Fe}(\text{NO})_2(\text{PAR}_3)_2$  as a function of (A) the Hammett parameter, and (B) the Brown-Okamoto constant  $\sigma_p^+$ .

Attempting to fit the data to a single trend line gives a slope of 0.11 with  $r^2 = 0.82$ ; a more reasonable fit results if two separate lines are used for the two groups. The slopes of the lines obtained are similar. The line obtained from the electron donating groups has a slope 0.047 with  $r^2 = 0.98$  while the line obtained for electron withdrawing groups had a slope of slope = 0.036 with a default  $r^2 = 1$  (since there are only two members of this group). Comparing only the *para* substituted compounds and leaving out the one *meta* substituted compound improves the fit for the electron donating groups and gives a slope = 0.049 with  $r^2 = 0.999$ . Parallel lines

similar to those described here and involving the same substituents on phenyl rings have been reported for a Hammett plot of the relative reactivities of *para*-substituted phenylacetyenes [67].

Hammett plots are known to give poor correlations when resonance factors are involved. Therefore an attempt was made to obtain a correlation between  $E^{\circ}$  and Brown-Okamoto constants as was done with the  $^{31}\text{P}$  NMR data (see earlier). No single linear correlation was found as shown in Figure 14b. The same two separate groups are present which seems to suggest that resonance is not a major factor separating the two groups.

#### 4.6 Infrared Spectroelectrochemistry

All of the studied compounds are easily oxidized to what are presumably  $[\text{Fe}(\text{NO})_2]^+$  containing species. The formation of each electrogenerated product is indicated by the appearance of two IR bands shifted to higher wave numbers relative to the neutral compound. Simultaneously, the two IR bands at lower wavenumbers which are associated with the neutral compound disappear.  $\Delta\nu_{\text{NO}}$  for each oxidation is approximately  $100\text{ cm}^{-1}$  which is an indication that the oxidations are metal centered.

The difference spectra for all compounds studied are similar except for the spectrum for **7**,  $\text{Fe}(\text{NO})_2(\text{P}(\text{C}_6\text{H}_4\text{-}i\text{-CF}_3)_3)_2$ . The IR bands for **7**<sup>+</sup> are not clearly defined and do not appear as symmetrical as those of the other compounds. This observation suggests that **7**<sup>+</sup> is short lived (perhaps releasing NO) compared to the other products on the time scale of the experiment.

The relative order of the  $\nu_{\text{NOS}}$  for product species is the same as that of the neutral compounds previously described. While as previously stated  $\Delta\nu_{\text{NO}}$  for each compound is approximately  $100\text{ cm}^{-1}$ , the antisymmetric stretches for the compounds containing the more

electron-donating substituents have larger  $\Delta\nu_{\text{NOS}}$  (by about  $4\text{ cm}^{-1}$ ) than the antisymmetric stretches of the compounds containing the more electron-withdrawing substituents.

As mentioned earlier, the cationic compound  $[\text{Fe}(\text{NO})_2(\text{PPh}_3)_2][\text{PF}_6]$  is known [33]; The  $\nu_{\text{NO}}$  of this compound ( $\nu_{\text{NO}} = 1766\text{ cm}^{-1}$  and  $1814\text{ cm}^{-1}$ ) is, as might be expected, comparable to  $4^+$  ( $\nu_{\text{NO}} = 1767\text{ cm}^{-1}$  and  $1816\text{ cm}^{-1}$ )

## 5. Conclusion

We set out to determine how the spectroscopic and electrochemical properties of the  $\text{Fe}(\text{NO})_2$  group are affected by small changes on the periphery of some dinitrosyliron diphosphine complexes (DNICs). We noted that determining this type of information was important because it will help provide a better understanding of the properties of the  $\text{Fe}(\text{NO})_2$  moiety. In pursuit of this goal we have successfully prepared a homologous series of six previously unpublished DNICs and characterized them by FTIR and  $^{31}\text{P}$  NMR spectroscopy, X-ray crystallography, cyclic voltammetry and fiber-optic IR spectroelectrochemistry.

Considering all of our results collectively, it was found that relatively small changes on the periphery of the DNICs do indeed have a major effect on their spectroscopic and electrochemical properties. We further report that the solvent system also has a noticeable influence. In addition, IR,  $^{31}\text{P}$  NMR spectroscopic and electrochemical data all show evidence of two different classes of  $\text{Fe}(\text{NO})_2\text{L}_2$  compounds (L = phosphine; those with electron withdrawing groups and those with electron donating groups at the phosphine periphery).

Specifically, with FTIR spectroscopy we showed that the  $\nu_{\text{NOS}}$  of our DNICs could be correlated with the phosphine ligand basicity as measured by the Hammett substituent parameter. We showed that in addition to the ligand basicity, the solvent donor and acceptor capacity

affected the  $\nu_{\text{NO}}$  as quantified by the Gutmann donor and acceptor numbers. We also showed that in  $\text{CH}_2\text{Cl}_2$  and in toluene, the compounds with electron donating groups could be distinguished from those with electron withdrawing groups. Such a distinction could not be made with the coordinating solvent acetonitrile, which suggested that the three different kinds of solvents interacted differently with each of the two classes of DNICs.

With the  $^{31}\text{P}$  NMR data, we showed that the phosphine chemical shifts are affected by the ligand basicity as exhibited by a two-line Hammett plot. Furthermore we obtained a linear relationship between  $\delta(^{31}\text{P})$  and the Brown-Okamoto constant suggesting that resonance factors also play some role, however, it is not clear how these factors are related or what other factors may be involved.

Substituent influenced structural differences are evident in the X-ray crystallographic data, but the changes are very small. However, on two extremes (most electron withdrawing substituents versus most electron donating substituents) the differences are quite clear. We were able to show that, among other small changes, the  $\text{Fe}(\text{NO})_2$  responds to the peripheral substituents by exhibiting an enhanced “*attracto*” conformation with electron withdrawing groups. Larger  $\text{O}\cdots\text{Fe}\cdots\text{O}$  angles found when electron donating groups are in place.

Lastly, the electrochemistry and the IR spectroelectrochemistry of the  $\text{Fe}(\text{NO})_2$  group is dramatically affected by small changes on the periphery of the DNICs. All of the compounds studied exhibit 1-electron oxidations. Reductions were not evident within the solvent potential limit, however, the parent  $\text{Fe}(\text{NO})_2(\text{CO})_2$  compound was easily reduced in a 1-electron process. Compounds containing the more basic phosphines were easily oxidized at lower  $E^\circ$  values while exhibiting a  $\Delta\nu_{\text{NO}}$  (compared to the neutral compound) of about  $100\text{ cm}^{-1}$ . Changing to less basic phosphines with more electron withdrawing substituents (e.g. *p*-F, *p*-Cl, *p*-CF<sub>3</sub>) shifted  $E^\circ$

values higher eventually leading to the short lived  $[\text{Fe}(\text{NO})_2(\text{P}(\text{C}_6\text{H}_4\text{-}p\text{-CF}_3)_3)_2]^+$  compound relative to the cyclic voltammetry time scale employed. Oxidation of **7**,  $\text{Fe}(\text{NO})_2(\text{P}(\text{C}_6\text{H}_4\text{-}p\text{-CF}_3)_3)_2$ , may even release NO as indicated by its IR difference spectrum.

All of the results herein can be used to emphasize the fact that the environment around DNICs affect their chemistry. This is true even from relatively remote positions on the molecule. As more is learned about the role of DNICs in biological systems including the local environment surrounding them (i.e. ligands), this information may be useful in helping to control their chemical fate and in predicting their derivatives.

## 6. Acknowledgments

We are grateful to the US Department of Education (GAANN Fellowship to MWJ; P200A030196), and the National Science Foundation (CHE-0076640 & CHE-0911537) for funding for this work. The authors also thank the National Science Foundation (CHE-0130835) and the University of Oklahoma for funds to acquire the diffractometer and computers used in this work. We are indebted to Dr. Lijuan Li (California State University, Long Beach, USA) for advice at the start of this project.

## 7. References

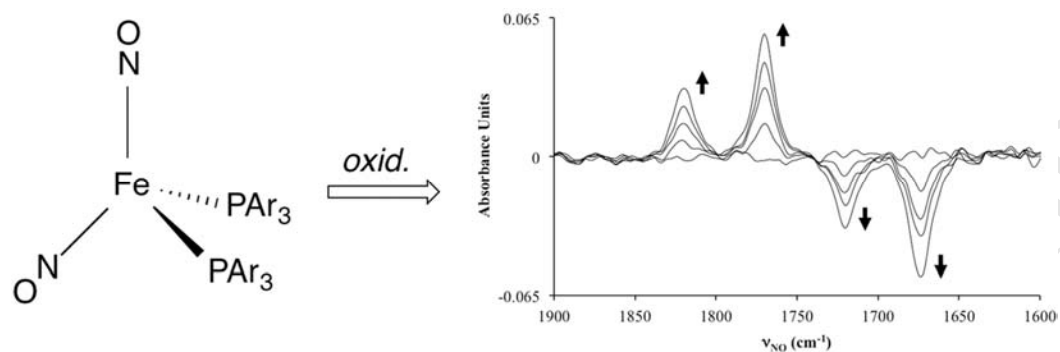
- [1] G.B. Richter-Addo, P. Legzdins, *Metal Nitrosyls*, Oxford University Press, New York, 1992.
- [2] J.L. Alencar, K. Chalupsky, M. Sarr, S.-K. V, A.F. Vanin, J.C. Stoclet, B. Muller, *Biochem. Pharmacol.* 66 (2003) 2365-2374.
- [3] A.F. Vanin, V.A. Serezhenkov, V.D. Mikoyan, M.V. Genkin, *Nitric Oxide* 2 (1998) 224-234.
- [4] A. Mulsch, P.I. Mordvintcev, A.F. Vanin, R. Busse, *Biochem. Biophys. Res. Commun.* 196 (1993) 1303-1308.
- [5] A. Mulsch, P. Mordvintcev, A.F. Vanin, R. Busse, *Febs Lett.* 294 (1991) 252-256.
- [6] A.F. Vanin, *FEBS Lett.* 289 (1991) 1-3.
- [7] A.F. Vanin, *Nitric Oxide* 21 (2009) 1-13.
- [8] H.L.K. Wah, M. Postel, M. Pierrot, *Inorg. Chim. Acta* 165 (1989) 215-220.
- [9] H.L.K. Wah, M. Postel, F. Tomi, *Inorg. Chem.* 28 (1989) 233-238.
- [10] V. Munyejabo, P. Guillaume, M. Postel, *Inorg. Chim. Acta* 221 (1994) 133-139.
- [11] M. Postel, F. Tomi, H.L.K. Wah, L. Mordenti, P. Guillaume, *Phosphorus Sulfur Silicon Relat. Elem.* 49 (1990) 453-457.
- [12] F. Tomi, H.L.K. Wah, M. Postel, *New J. Chem.* 12 (1988) 289-292.
- [13] J.P. Candlin, W.H. Janes, *J. Chem. Soc. C* (1968) 1856-1860.
- [14] G.E. Gadd, M. Poliakoff, J.J. Turner, *Organometallics* 6 (1987) 391-397.
- [15] D. Huchette, J. Nicole, F. Petit, *Tetrahedron Lett.* (1979) 1035-1038.
- [16] D. Ballivet-Tkatchenko, C. Esselin, J. Goulon, *J. Phys. (France)* 47 (1986) 343-346.
- [17] P.L. Maxfield, *Dimerization of Diolefins*, U.S. Patent 3,377,397. April 9, 1968.

- [18] L. Li, G.D. Enright, K.F. Preston, *Organometallics* 13 (1994) 4686-4688.
- [19] C. Pellat, Y. Henry, J.C. Drapier, *Biochem. Biophys. Res. Comm.* 166 (1990) 119-125.
- [20] J.R. Lancaster, J.B. Hibbs, *Proc. Nat. Acad. Sci. U.S.A.* 87 (1990) 1223-1227.
- [21] D. Reddy, J.R. Lancaster, D.P. Cornforth, *Science* 221 (1983) 769-770.
- [22] E. Cesareo, L.J. Parker, J.Z. Pedersen, M. Nuccetelli, A.P. Mazzetti, A. Pastore, G. Federici, A.M. Caccuri, G. Ricci, J.J. Adams, M.W. Parker, M. Lo Bello, *J. Biol. Chem.* 280 (2005) 42172-42180.
- [23] A.F. Vanin, G.B. Menshikov, I.A. Moroz, P.I. Mordvintcev, V.A. Serezhenkov, D.S. Burbaev, *Biochim. Biophys. Acta* 1135 (1992) 275-279.
- [24] J.C. Toledo, C.A. Bosworth, S.W. Hennon, H.A. Mahtani, H.A. Bergonia, J.R. Lancaster, *J. Biol. Chem.* 283 (2008) 28926-28933.
- [25] J. Stadler, H.A. Bergonia, M. Disilvio, M.A. Sweetland, T.R. Billiar, R.L. Simmons, J.R. Lancaster, *Arch. Biochem. Biophys.* 302 (1993) 4-11.
- [26] L. Li, N. Reginato, M. Urschey, M. Stradiotto, J.D. Liarakos, *Can. J. Chem.* 81 (2003) 468-475.
- [27] L. Li, *Comments Inorg. Chem.* 23 (2002) 335-353.
- [28] A. Horsken, G. Zheng, M. Stradiotto, C.T.C. McCrory, L. Li, *J. Organomet. Chem.* 558 (1998) 1-9.
- [29] V.G. Albano, A. Araneo, P.L. Bellon, G. Ciani, Manasser.M, *J. Organomet. Chem.* 67 (1974) 413-422.
- [30] V. Munyejabo, J.P. Damiano, M. Postel, C. Bensimon, J.L. Roustan, *J. Organomet. Chem.* 491 (1995) 61-69.

- [31] A.E. Gerbase, E.J.S. Vichi, E. Stein, L. Amaral, A. Vasquez, M. Horner, C. Maichle-Mossmer, *Inorg. Chim. Acta* 266 (1997) 19-27.
- [32] T.E. Bitterwolf, B. Steele, *Inorg. Chem. Commun.* 9 (2006) 512-513.
- [33] F.L. Atkinson, H.E. Blackwell, N.C. Brown, N.G. Connelly, J.G. Crossley, A.G. Orpen, A.L. Rieger, P.H. Rieger, *J. Chem. Soc., Dalton Trans.* (1996) 3491-3502.
- [34] D. Ballivet, C. Billard, I. Tkatchenko, *Inorg. Chim. Acta* 25 (1977) L58.
- [35] S. Pignataro, G. Distefano, A. Foffani, *J. Am. Chem. Soc.* 92 (1970) 6425-6429.
- [36] J.J. Eisch, R.B. King, *Metal Nitrosyl Derivatives*, In *Organometallic Syntheses*, Academic Press, New York, 1965, pp 167-168.
- [37] M.J. Shaw, R.L. Henson, S.E. Houk, J.W. Westhoff, M.W. Jones, G.B. Richter-Addo, *J. Electroanal. Chem.* 534 (2002) 47-53.
- [38] D.W. McBride, S.L. Stafford, F.G.A. Stone, *Inorg. Chem.* 1 (1962) 386-388.
- [39] P. van der Sluis, A.L. Spek, *Acta Cryst.* A46 (1990) 194-201.
- [40] M.W. Jones, D.R. Powell, G.B. Richter-Addo, *Acta Cryst.* E67 (2011) M331.
- [41] M.W. Jones, D.R. Powell, G.B. Richter-Addo, *Acta Cryst.* E67 (2011) M332.
- [42] M.W. Jones, D.R. Powell, G.B. Richter-Addo, *Acta Cryst.* E67 (2011) M247.
- [43] C.-H. Hsieh, M.Y. Darensbourg, *J. Am. Chem. Soc.* 132 (2010) 14118-14125.
- [44] T. Allman, R.G. Goel, *Can. J. Chem.* 60 (1982) 716-722.
- [45] A. Neubrand, A.J. Poe, R. van Eldik, *Organometallics* 14 (1995) 3249-3258.
- [46] W. Hieber, H. Fuhrling, *Z. Anorg. Allg. Chem.* 373 (1970) 48-56.
- [47] G. Piazza, G. Paliani, *Z. Phys. Chem. (Frankfurt)* 71 (1970) 91-101.
- [48] F.T. Tsai, S.J. Chiou, M.C. Tsai, H.W. Huang, M.H. Chiang, W.F. Liaw, *Inorg. Chem.* 44 (2005) 5872-5881.

- [49] C.A. Tolman, *J. Am. Chem. Soc.* 92 (1970) 2956-2965.
- [50] C.A. Tolman, *J. Am. Chem. Soc.* 92 (1970) 2953-2956.
- [51] C.A. Tolman, *Chem. Rev.* 77 (1977) 313-348.
- [52] J. Lewis, R.J. Irving, G. Wilkinson, *J. Inorg. Nucl. Chem.* 7 (1958) 32-37.
- [53] A. Foffani, A. Poletti, R. Cataliotti, *Spectrochim. Acta A24* (1968) 1437-1447.
- [54] V. Gutmann, *Monatsh. Chem.* 108 (1977) 429-435.
- [55] J. W. D. Horrocks, R.H. Mann, *Spectrochim. Acta* 21 (1965) 399-408.
- [56] C. Hansch, A. Leo, R.W. Taft, *Chem. Rev.* 91 (1991) 165-195.
- [57] L.P. Hammett, *Chem. Rev.* 17 (1935) 125-136.
- [58] M.B. Smith, J. March, *March's Advanced Organic Chemistry 5th Ed.*, John Wiley & Sons, New York, 2001, pp. 368-380.
- [59] U. Mayer, V. Gutmann, W. Gerger, *Monatsh. Chem.* 106 (1975) 1235-1257.
- [60] V. Gutmann, *Electrochim. Acta* 21 (1976) 661-670.
- [61] V. Gutmann, *Coord. Chem. Rev.* 18 (1976) 225-255.
- [62] V. Gutmann, E. Wychera, *Inorg. Nucl. Chem. Lett.* 2 (1966) 257-260.
- [63] J.R. Chipperfield, *Oxford Chem. Primers* 69 (1999).
- [64] Y. Marcus, *Chem. Soc. Rev.* 22 (1993) 409-416.
- [65] H.C. Brown, Y. Okamoto, *J. Am. Chem. Soc.* 80 (1958) 4979-4987.
- [66] L. Hedberg, K. Hedberg, S.K. Satija, B.I. Swanson, *Inorg. Chem.* 24 (1985) 2766-2771.
- [67] S.I.M. Paris, F.R. Lemke, *Inorg. Chem. Commun.* 8 (2005) 425-428.

## Graphical Abstract

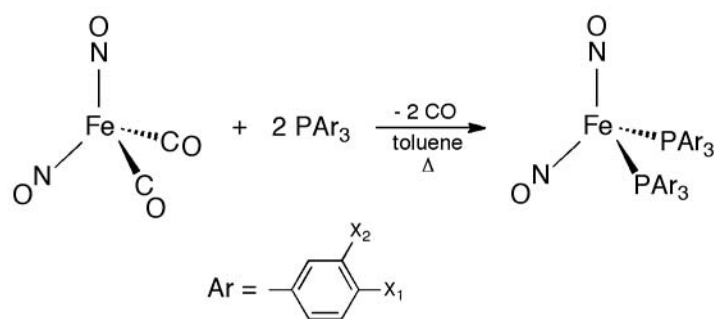


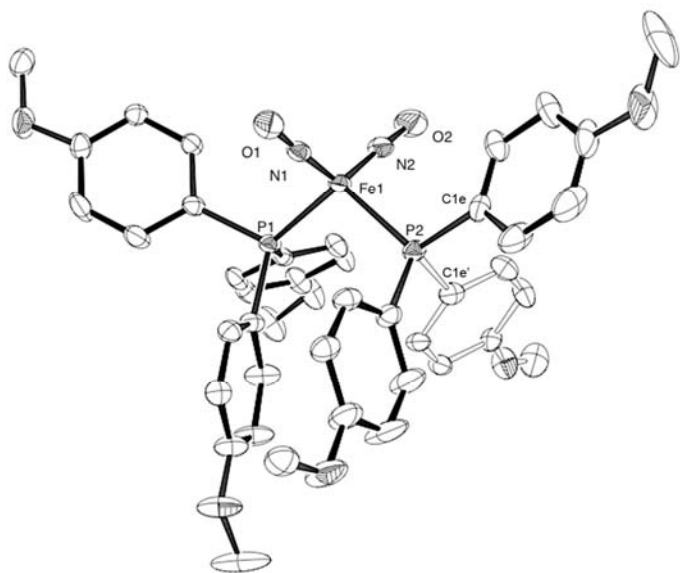
### Graphical Abstract Synopsis:

Dinitrosyl iron complexes (DNICs) are important in biology and have utility in chemical catalysis. Several new DNICs of the form  $\text{Fe}(\text{NO})_2(\text{PAr}_3)_2$  ( $\text{PAr}_3$  = triarylphosphine) have been prepared and characterized by spectroscopy and X-ray crystallography. The results of the spectroscopy and electrochemistry reveal subtle substituent effects upon phosphine variation.

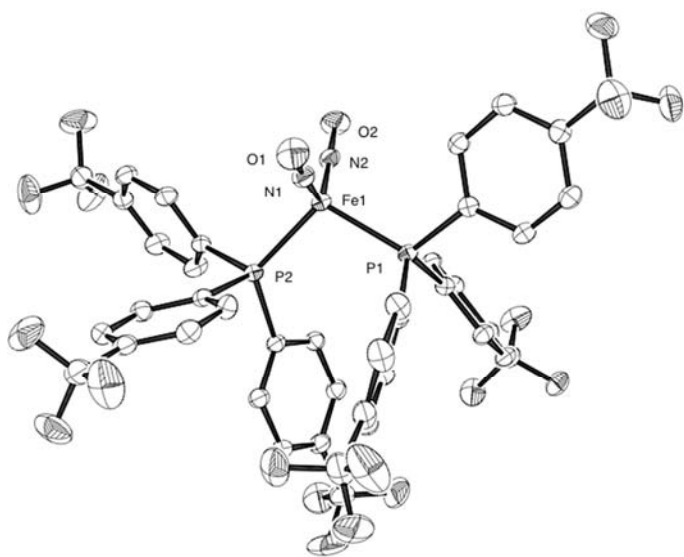
### Highlights:

1. New dinitrosyl iron complexes with phosphine ligands have been prepared.
2. X-ray crystallography reveals essentially linear FeNO linkages in these compounds.
3. Phosphine substitutions have effects on the spectroscopy and electrochemistry.
4. Infrared spectroelectrochemistry reveals metal-centered oxidations.

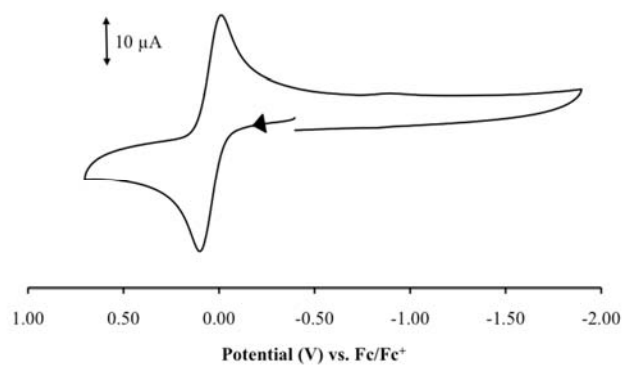




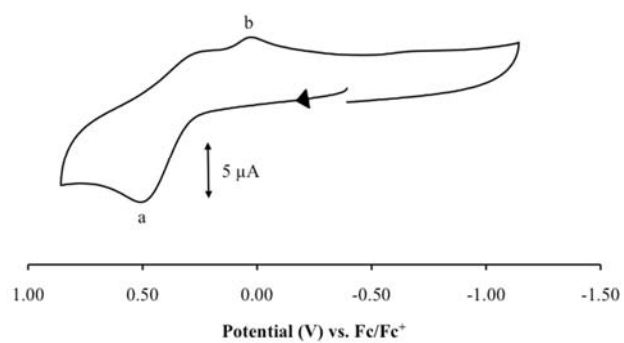
ACCEPTED MANUSCRIPT

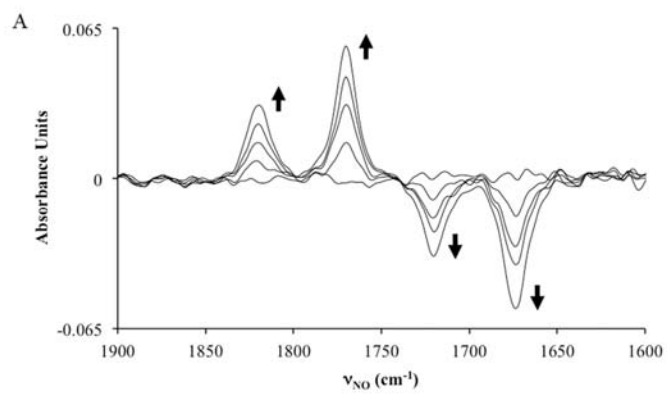


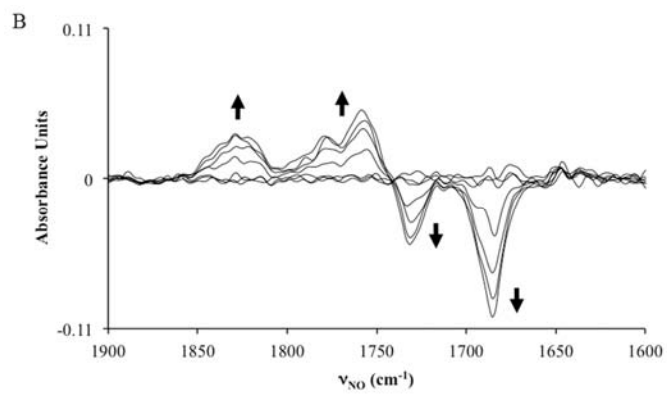
ACCEPTED MANUSCRIPT

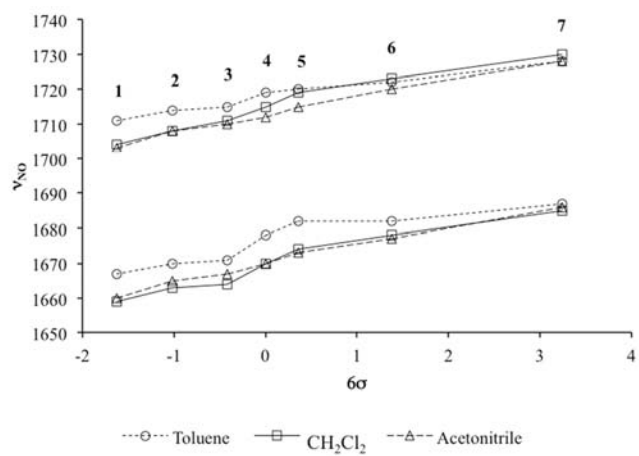


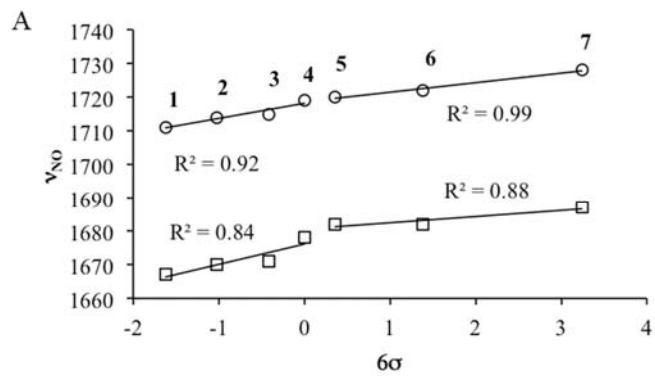
ACCEPTED MANUSCRIPT

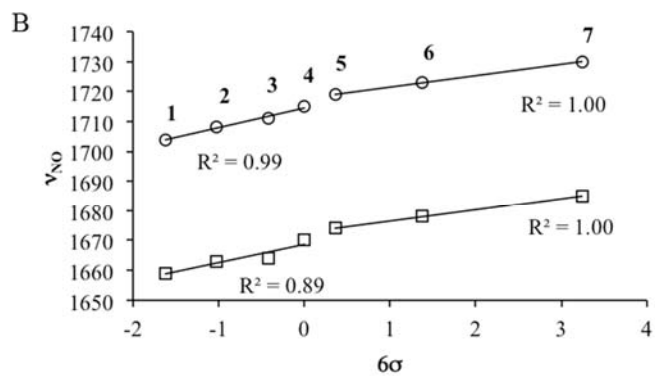


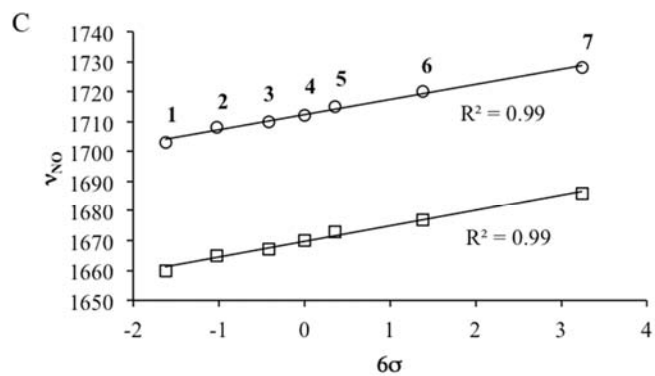


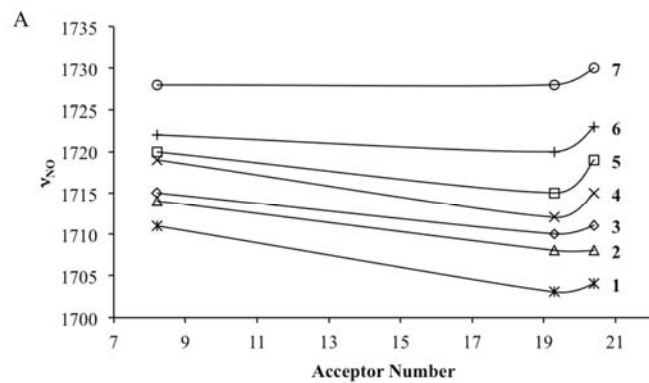


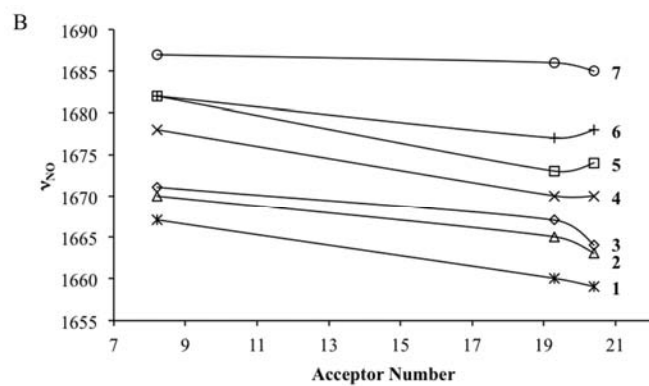


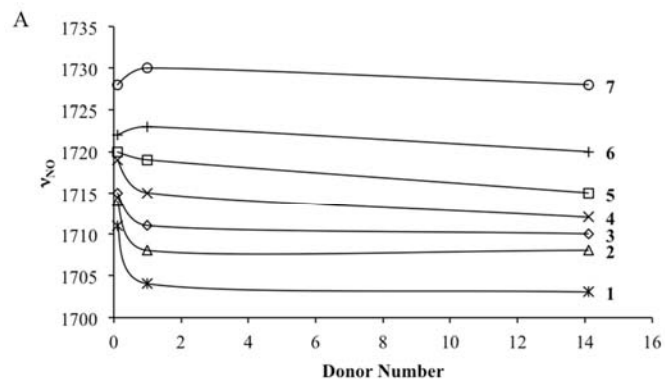


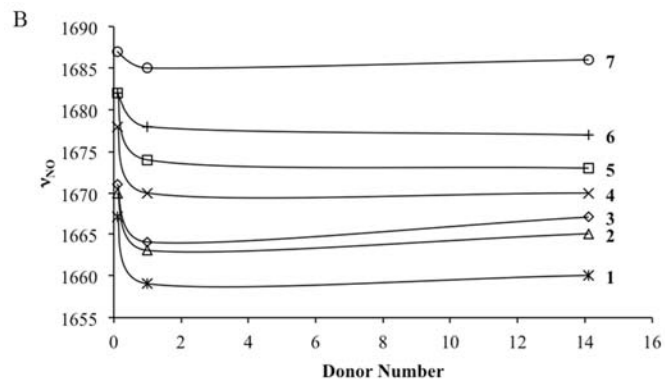


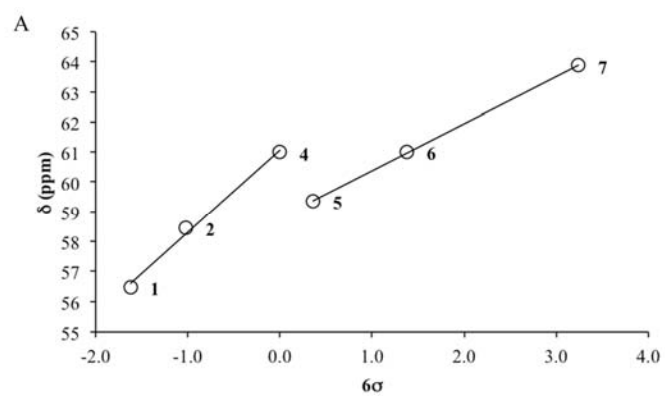


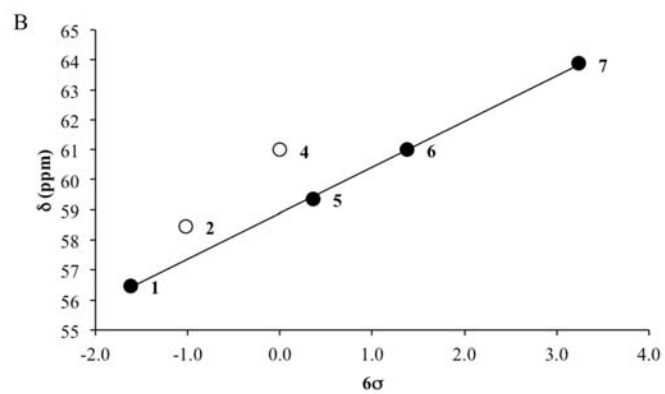


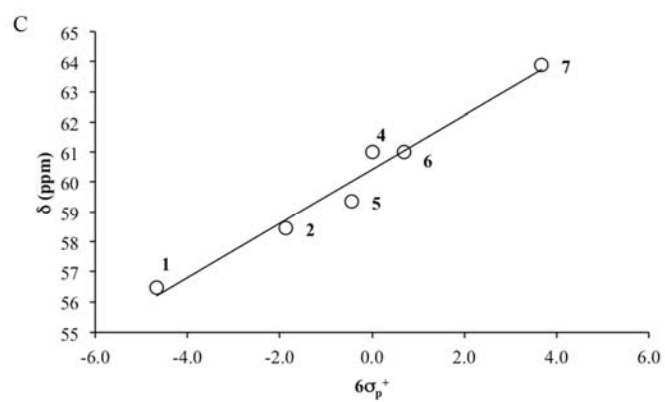


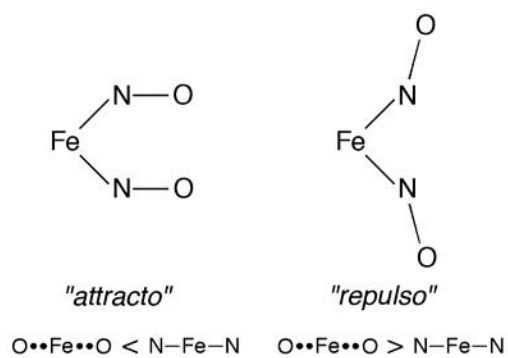












ACCEPTED MANUSCRIPT

